Politecnico di Milano

School of Industrial and Information Engineering

Master of Science in Telecommunication Engineering

Department of Electronics, Information and Bioengineering

POLITECNICO
MILANO 1863

COVERAGE, INTERFERENCE AND POWER CONSUMPTION ANALYSIS OF AN AERIAL BASE STATION IN CASE OF DRONE ASSISTED DEVICE-TO-DEVICE COMMUNICATIONS

Supervisor: Prof. Maurizio Magarini

Co-supervisor: Dr. Navuday Sharma

Thesis of:

Daniele Giovanni Cileo ID. 837802

Academic Year 2016–2017

Acknowledgments

A special thank goes to my friend Navuday Sharma who teach me many things and help me a lot in developing the whole work. Thanks also to my best friend Alessandro for having pushed me in giving the best and for having taken me out sometimes for a game of pool.

Abstract

Unmanned Aerial Vehicles (UAV), commonly known as drones, have been used as a low altitude platforms for many purposes. Initially they were used for military purposes, like surveillance or reconnaissance activities. Currently, they have received enormous interest in civil applications too, like search and rescue, weather detection, wildlife monitoring, farming, film making etc. With the upcoming 5G technology of base stations mounted on aerial platforms, such as UAVs, Helikite, Aerostats etc., the issues of coverage area, capacity, interference and power consumption are of massive importance in the context of cellular network. The aim of this thesis is to analyze and solve these problems, by processing data generated using a ray tracing and wireless electromagnetic propagation simulations tool called "Wireless Insite" by Remcom. Moreover, the variation in coverage area is analyzed, as a result of the inter-cell interference with respect to the movement of the UAV and its variation in height in the range between 100 m and 2000 m, on the basis of traffic intensity generated by uniformly distributed users on the ground. Three different propagation scenarios are considered: suburban, urban and urban high rise. Also, the optimal height of the aerial base station for a transmitted power of 18 dBm is identified to maximize the coverage percentage value. Then, an aerial base station power consumption analysis is done, to get the best transmitted power as a tradeoff between total consumed power and coverage percentage. Finally, the case of using an aerial base station in the case of drone-assisted Device-to-

Device (D2D) communication is taken into account. A best and worst case is identified and a solution is proposed for the movement of the UAV to obtain the benefit of full coverage over partial coverage for a D2D user.

Sommario

Gli aeromobili a pilotaggio remoto (APR o UAV), comunemente conosciuti come droni, sono al giorno d'oggi largamente utilizzati come piattaforme aeree a bassa quota (LAPs) per gli scopi più svariati. Inizialmente, essi erano utilizzati esclusivamente per scopi militari come operazioni di sorveglianza o attività di ricognizione. Recentemente, hanno riscosso un enorme interesse anche in applicazioni civili, come operazioni di ricerca e salvataggio, rilevamenti meteo, monitoraggio della fauna selvatica, attività agricole, film making etc. Con l'imminente tecnologia 5G di base stations montate su piattaforme aeree, come UAVs, piccoli palloni aerostatici o droni, la copertura, la capacità, l'interferenza ed il consumo di potenza sono argomenti di rilevante importanza e considerazione per le reti cellulari. L'obiettivo della tesi è analizzare queste problematiche, gestendo i dati generati tramite un software di ray tracing chiamato "Wireless Insite" offerto da Remcom. Inizialmente, viene analizzata la variazione in copertura, come risultato dell'interferenza tra celle adiacenti rispetto al movimento dell'UAV e la sua variazione in altezza (da 100 a 2000 m), sulla base del traffico generato da utenti uniformemente distribuiti. Per fare questo, si considerano tre differenti scenari di propagazione: suburbano, urbano ed urbano in presenza di grattacieli. Inoltre, viene individuata l'altezza massima della base station aerea affinché la percentuale di copertura, nel caso in cui venga trasmessa una potenza pari a 18 dBm, sia massimizzata; particolare attenzione è riservata al consumo di potenza di una base station aerea. In

conclusione, si considera il caso in cui si usi una stazione base aerea per una comunicazione Device-to-Device (D2D). Il caso ottimo e il caso pessimo sono analizzati e viene proposta una soluzione che permette di passare da una situazione di copertura parziale a una totale, con tutti i benefici del caso.

List of Abbreviations

3GPP	Third Generation Partnership Project
4G	Fourth Generation
5G	Fifth Generation
A2G	Air-to-Ground
ABS	Aerial Base Station
ACK	Acknowledgement
AWGN	Additive White Gaussian Noise
BS	Base Station
D2D	Device-to-Device
DCI	Downlink Control Information
DL	Downlink
DNS	Domain Name System
DOA	Direction of Arrival
EIRP	Equivalent Isotropic Radiated Power
E.M.	Electromagnetic

eNB	E-UTRAN Node B
EPC	Evolved Packet Core
FDD	Frequency Division Duplex
GS	Ground Station
HARQ	Hybrid Automatic Repeat Request
HR	High Rise
HSS	Home Subscriber Server
HTTP	HyperText Transfer Protocol
IP	Internet Protocol
ITU-R	International Telecommunications Union-Radiocommunication
LAP	Low Altitude Platform
LTE	Long Term Evolution
LTE-A	Long Term Evolution Advanced
LOS	Line of Sight
MAC	Media Access Control
MANET	Mobile Ad Hoc Network
MIB-SL	Sidelink Mater Information Block
MUSIC	Multiple Signal Classification
ESPRIT	Estimation of Signal Parameters via Rotational Invariance Technique

NACK	Negative Acknowledgement
NLOS	Non Line of Sight
PDCP	Packet Data Convergence Protocol
PDU	Protocol Data Unit
PL	Path Loss
PLE	Path Loss Exponent
PLMN	Public Land Mobile Network
PRB	Physical Resource Block
ProSe	Proximity Services
PSBCH	Physical Sidelink Broadcast Channel
PSCCH	Physical Control Channel
PSDCH	Physical Downlink Shared Channel
PSSCH	Physical Sidelink Shared Channel
PSSS	Primarly Synchronization Signal
QoS	Quality Of Service
RACH	Random Access Channel
RB	Resource Block
RLC	Radio Link Control
RP	Resource Pool
RRC	Radio Resource Control

RSRP	Reference Signal Received Power
SBCCH	Sidelink Broadcast Control Channel
SC	Sidelink Control
SC-FDMA	Single Carrier Frequency-Division Multiple Access
SCI	Sidelink Control Information
SFN	System Frame Number
SIB	System Information Block
SINR	Signal-to-Interference-Plus-Noise Ratio
SIR	Signal-to-Interference Ratio
SL	Sidelink
SLP	Secure User Plane Location
SL-BCH	Sidelink Broadcast Channel
SL-SCH	Sidelink Shared Channel
SLSS	Sidelink Synchronization Signal
SNR	Signal-to-Noise Ratio
S-RSRP	Sidelink Reference Signal Received Power
SSSS	Secondary Synchronization Signal
STCH	Sidelink Traffic Channel
TA	Timing Advance
thr	Threshold

TOA	Time of Arrival
TDD	Time Division Duplex
UAV	Unmanned Aerial Vehicle
UE	User Equipment
UL	Uplink
ULA	Uniform Linear Array
USIM	Universal Subscriber Identity Module

Contents

List of Figures

List of Tables

Introduction

Many years have passed since the launch of UAVs, such as drones or small airplanes, being used in many different activities. An Unmanned aerial vehicle (UAV) is defined as a "powered aerial vehicle that does not carry a human operator, uses aerodynamic forces to provide vehicle lift, can fly autonomously or be piloted remotely, can be expendable or recoverable and can carry a lethal or non-lethal payload". Initially, in fact, they were massively and exclusively used for military purposes, like surveillance or patrolling activities in delicate war zones. Nowadays, this topic is becoming of enormous interest in different scenarios for many companies, that are investing a lot in this field. Using flying vehicles, instead of man power, to help humans in their daily activities both for civil purposes and public safety activities, like agriculture, recreational purposes, products delivery (as the famous trading company "Amazon" has studied first), photography and many others is now considered massively important. Recently, the idea of using flying vehicles to install base stations on them, with the aim of getting an increment in cellular networks capacity and coverage, reducing the effects of interference or offering connectivity to affected users in case of emergency after natural disasters (such as earthquake, hurricanes, tsunami etc.) when terrestrial architecture is down, is becoming a point of big interest and it could become a big improvement for telecommunications technologies in the next few years; this is also our point of interest and analysis.

Figure 1: An example of an aerial base station quadcopter from NOKIA working at 4G

The studies that have been done consider both the case of fixed-wings UAVs like small airplanes to fly over big area and rotary UAVs; for the purposes of this thesis, we have assumed to use rotary UAV because they can be moved in a much easier way but, above all, they can stay still in a point while flying (that a fixed wing airplane cannot do) with the possibility of offering a specific coverage and maintaining an optimal height value. In this thesis, we will explain how to face the problem with the aim of offering an innovative analysis of the coverage area, capacity and intercell-interference. Since it is a new field of research, few people have investigated in this direction and all of them have based their conclusions on analytical results only. In this direction, our work will bring novelty because it is based on simulations results of a Ray-tracing software called *Wireless Insite*. An aerial base station (ABS) at different heights (from 100 m to 2000 m) is simulated, considering a specific micro cellular cell of 200 m of radius where the users are uniformly distributed in three different scenarios (suburban, urban and urban high rise). The goal is to understand what is the

impact of the height of the drone on the coverage, keeping the ABS fixed in the center of the simulation scenario, with the aim of individualizing an optimal value for maximizing coverage and minimizing the overall power consumption. Moreover, power consumption for an ABS is investigated, considering both the power needed to the UAV to fly and the transmitted power to the user equipments (UEs). The last part will be centered on the use of ABS in the Device-to-Device (D2D) communication, to verify if it is possible to use a drone for direct discovery and direct communications. Moreover, a possible solution is proposed to switch from the case of partial coverage to the case of full coverage, where no synchronization signals or dedicated architecture is needed, by moving the ABS in a different position; some conclusions on the worst and best cases are offered, reflecting on how it is important the impact of the power on the coverage area so that the D2D communication can be established with the lowest impact on the UEs energy consumption.

Chapter 1 and Chapter 2 contains the state-of-art regarding basis of propagation phenomena that can be encountered along the propagation of E.M. fields along the path from Tx to Rx. Chapter 3 contains the coverage, capacity and interference analysis and results in the case of an ABS fixed at the center of the cell. Moreover, a complete power consumption analysis can be found at the end of the chapter. Chapter 4, contains the analysis and feasibility studies in the case of a drone-assisted Device-to-Device communication among two UEs on the ground. Nevertheless, a solution to switch from a partial-coverage to a full-coverage situation by moving the ABS is proposed.

The results contained in the third chapter have been published in a paper at the 14th International Symposium on Wireless Communication Systems (*ISWCS 2017*) conference with the title "Coverage, Capacity and Interference Analysis for an Aerial Base Station in Different Environments"; the authors of the above paper are: Daniele Giovanni Cileo (*daniele.cileo@mail.polimi.it*),

Navuday Sharma (*navuday.sharma@polimi.it*) and Maurizio Magarini (*maurizio.magarini@polimi.it*).

Chapter 1

Propagation Basics

1.1 Introduction

For understanding the propagation basics, it is important to describe how a communication between a transmitter and a receiver takes place and which are the propagation mechanisms that occur. A statistical description of the propagation channel and a specific classification of the phenomena that are encountered every time a radio wave is propagating along the channel is provided. Thanks to the measurements that could be done when a propagation occurs, it is possible to offer a precise statistical characterization of the channel and create useful generalized models. Moreover, since the communication between a transmitter and a receiver in a wireless environment largely depends on the propagation channel, it is important to give a precise description and characterization of the possible propagation phenomena and mechanisms.

1.2 Free Space Path Loss: The Simplest Propagation Model

The ideal case of propagation is the one where an electromagnetic wave propagates in the free space, *i.e.* in absence of obstacles, such as walls, terrain, buildings and other objects, in line of sight conditions (LOS). Since the environment is ideal and empty, the only form of attenuation here is represented by the attenuation due to the distance; the greater the distance, the higher the attenuation the wave encounters (*i.e.* as distance increases, the wave is attenuated). The case of free space path loss between transmitter and receiver is described by the Friis formula.

The $EIRP$ is defined as the equivalent isotropic radiated power of a transmitter radiating a power P_t through an antenna of transmission gain G_t; alternatively, it could be defined as the power produced by an isotropic antenna with peak power density in the direction of maximum gain. It is defined as:

$$EIRP = P_t G_t \tag{1.1}$$

At receiver side, the effective area A_e is defined as the area that is available at the receiver to capture the signal coming from the transmitter. It is a function of the gain of the receiver antenna G_r, the wavelength λ of the transmitted signal and is defined as follows:

$$A_e = \frac{\lambda^2 G_r}{4\pi} \tag{1.2}$$

After defining both the $EIRP$ and the effective area A_e, it is possible to get the Friis relation, defining the received power P_r at distance d from the transmitter as:

$$P_r = EIRP \times A_e = P_t G_t G_r \left(\frac{\lambda}{4\pi d}\right)^2, \tag{1.3}$$

remembering that the ratio $\frac{P_t G_t}{4\pi d^2}$ is defined as the power density S at distance d from the transmitter.

Finally, it is interesting to identify the attenuation term inside the Friis equation due to pathloss, which is defined as $PL = \left(\frac{\lambda}{4\pi d}\right)^2$: it represents the amount of attenuation that the signal has after having propagated for a length d [16].

1.3 Propagation Phenomena

During the propagation of a radio wave along the communication channel, a variety of phenomena can be encountered. In the following subsections, a precise and detailed classification and description is given for the most important cases: reflection, diffraction, scattering, shadowing and multipath fading [16].

1.3.1 Reflection, Absorption and Refraction

When a radio wave that is propagating from the transmitter to the receiver encounters a smooth surface, large compared to the wavelength, it is reflected; in fact, a portion of the wave is transmitted to the receiver and another portion is reflected back to the same medium. The property that guides this phenomenon is the fact that, denoting with ϑ_i the angle of incidence and ϑr the angle of reflection, the two angle are equal:

$$\vartheta_i = \vartheta_r \tag{1.4}$$

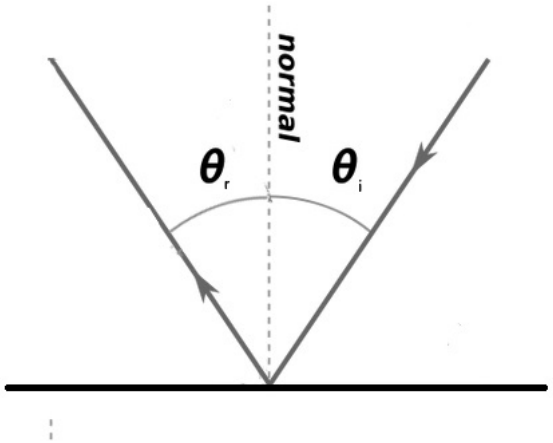

Figure 1.1: The reflection law

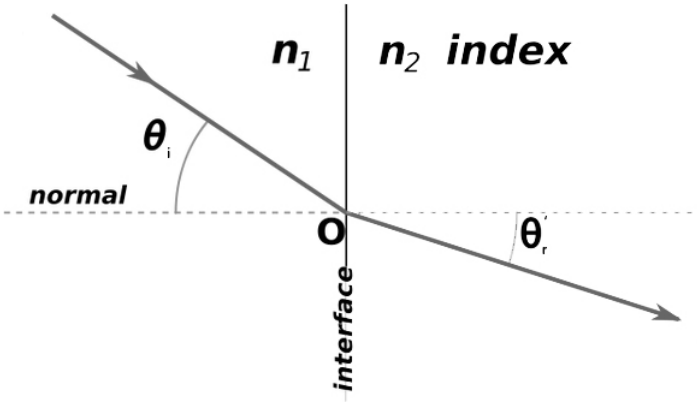

Figure 1.2: The Snell's law

Sometimes, it happens that part of the signal strength is lost as a result of the wave passing through a dark or opaque medium; this is what is called *absorption* (*i.e.* the signal is neither reflected nor refracted).

Moreover, the signal can encounter different layers (i.e different materials with different refractive index $n_2 < n_1$) and change its velocity; thus, the signal will bend of a certain angle ϑ'_r. This is what is called *refraction* and it is regulated by the Snell's law [16]:

$$n_1 \sin \vartheta_i = n_2 \sin \vartheta'_r \tag{1.5}$$

1.3.2 Ray Tracing Propagation Modeling

Ray tracing models are largely used to simulate and approximate the propagation of a radio wave, according to the Maxwell's equations, with the big advantage of not solving them. The idea is to approximate the wavefronts as simple particles and analyze the impact that effects like reflections, refractions have on the signal strength, ignoring the more complex phenomenon of scattering due to rough surfaces, that is predicted using Maxwell's coupled differential equations. These models can be considered as accurate models when the number of multipath components is small and the exact environment in which the communication takes place is known. Moreover, they heavily depend on the geometry and dielectric properties of the environment through which the signal is propagating. The simplest known model is called the *two-ray model;* it is used to characterize the easiest case in which the received signal is composed of two parts: the first one due to the LOS component and a second one due to the reflection by the ground of the transmitted signal (NLOS, non line of sight). The signals are modeled as rays to be able to describe the propagation in the scenario. Considering a transmitter of height h_t and a receiver of height h_r at a distance d one from the other, we can represent the two-ray model as in Figure 1.3. There are two components arriving at receiver at different instants of time; the first one is propagating in LOS condition through a distance d_{dir}, the second one is the reflected wave that is propagating in NLOS condition through a distance $d_{ref} > d_{dir}$ [39].

1.3.3 Diffraction and Knife-Edge Effects

Another possible phenomenon that a radio wave can encounter when propagating along a propagation scenario is *diffraction.* More specifically, it happens every time a radio wave encounters a sharp edge (like the edge of a building

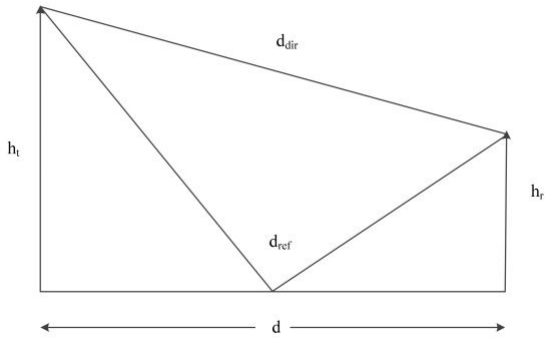

Figure 1.3: The two-ray model

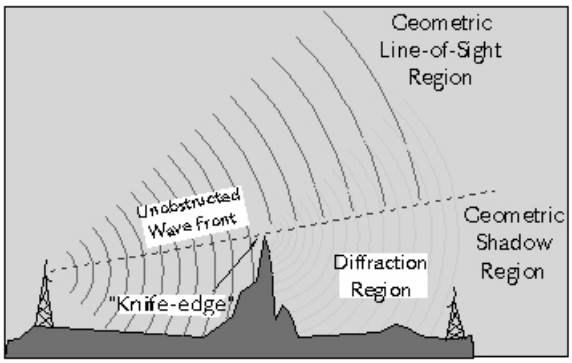

Figure 1.4: The knife-edge effect

such as rooftops or the edge of a hill), and it is based on the Huygens principles that state the fact that each point of the wavefront is a new source of spherical wavefronts in the direction of propagation. The effect of a reflection is described as a bending of the propagating wave around the corner of an obstacle and the consequent propagation of the wave in the region behind the obstacle, as shown in Figure 1.4.

In wireless communications, the case of diffraction, *i.e.* the redirection and bending of the electromagnetic wave by the buildings and obstacles present in the propagation scenario and the propagation of the bent wave in the geometric shadow region of obstacle, is called *knife-edge effect* [21] [16].

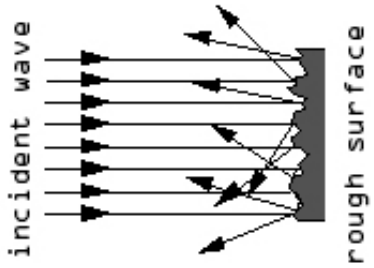

Figure 1.5: The scattering effect at a rough surface

1.3.4 Scattering Effects

When a propagating wave encounters a rough surface of an object that has a size comparable to the wavelength λ of the incident signal, the phenomenon that is occurring is called *scattering*; the effect is translated into a reflection of the incident wave in many different directions, with different angles and different phases since the surface is uneven. It is worth noting that as the surface roughness increases the amount of scattering increases too, and so the amount of energy of every reflected component is reduced. To analyze the roughness of a surface the Rayleigh criterion is used [39]:

$$\Delta h = \frac{\lambda}{8 cos \vartheta_i} \tag{1.6}$$

where Δh is the deviation in height, λ is the wavelength and ϑ_i is the angle of incidence; the surface can be considered as rough if the deviation is greater than $\frac{\lambda}{8}$.

1.3.5 Shadowing Effects

Since the propagation of a radio wave can take place in different type of environments, many of the latter phenomena could be encountered by the signals; this is the reason why, the pathloss, at a given distance d, will experience random variation due to the presence of objects along the signal path (*i.e.* a

specific deviation from the ideal case of free space communication), known as *shadowing* or *shadow fading*, that will affect the strength of all the components of the signal moving toward the receiver. The variation in the pathloss, is a Gaussian distributed random variable with standard deviation σ, that represents the shadowing effect in the pathloss. Statistical models are commonly used to characterize the random attenuation; in the case of shadowing a *log-normal distribution* is used [21] [16]:

$$p(\psi) = \frac{\zeta}{\sqrt{2\pi}\sigma_{\psi dB}\psi} \exp\left[-\frac{(10\log_{10}\psi - \mu_{\psi dB})^2}{2\sigma^2_{\psi dB}}\right] \quad , \psi > 0 \tag{1.7}$$

where ψ is the pathloss, assumed to be random (*i.e.* $\psi_{dB} = 10\log_{10}\psi$ is the pathloss in dB), $\xi = \frac{10}{\ln 10}$, $\mu_{\psi dB}$ is the mean value of ψ_{dB} and $\sigma_{\psi dB}$ is the standard deviation of ψ_{dB}.

1.4 Fading

In wireless communication, *fading* represents the random attenuation in the pathloss that is changing due to multiple propagation phenomena such as reflections, refractions, diffractions or scattering; this is what is called *large-scale fading*. Nevertheless, there are many other important phenomena to be described and analyzed that have a big impact on the received signal; they can be grouped together as small *scale fading effect*s.

1.4.1 Multipath Fading

The first impact is due to the presence of the multipath fading. It refers to the random fluctuations in the received signal due to the presence of multipath components of the signal that arrive at receiver side with different phases (*i.e.* different travel time for each component), directions and field strength,

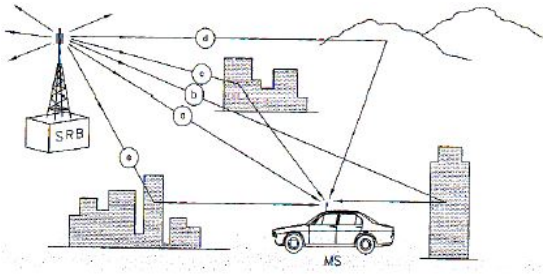

Figure 1.6: The multipath fading

depending on the path each component has traveled and how many phenomena (reflections, diffractions, scattering and shadowing) has encountered along the propagation channel. Moreover, LOS components will have a higher energy because they will not encounter any obstacles along the path, that instead will encounter the NLOS components which will have a lower signal strength and a larger distance to be travelled. The total field will be the combinations of LOS and NLOS components and it can be constructive of destructive depending on the phases value; hence, the total field could increase or decrease depending on these factors. The total received signal can be expressed as [21] [16]:

$$s_R(t) = \sum_{k=i}^{N} a_k \cos\left(2\pi f_0 t + \varphi_k\right) \tag{1.8}$$

where φ_k is the relative phase of each component, N is the number of replicas, a_k is the amplitude of each component and f_0 is the signal frequency.

Two main types of fading distributions can be identified to characterize the small fading effect: Rayleigh and Rician distribution.

1.4.1.1 Rayleigh Distribution

It is used to characterize small-scale fading of signals in case of an infinite number of adjacent paths, without the presence of a dominant component (*i.e.* the values of the amplitudes a_k are comparable and there is no LOS component at the receiver side) and casual phases value, uniform in the range

$[0, 2\pi]$. The probability density function and the cumulative density function of the Rayleigh distribution of a random variable x can be expressed as [21] [16]:

$$f_p(x) = \begin{cases} \frac{1}{2\sigma^2} \exp\left(-\frac{x}{2\sigma^2}\right), & 0 \leq x \leq \infty, \\ 0, & elsewhere, \end{cases} \tag{1.9}$$

and

$$F_p(x) = 1 - \exp\left(-\frac{x}{2\sigma^2}\right), \tag{1.10}$$

respectively.

1.4.1.2 Rician Distribution

It is used when the Rayleigh assumptions are not verified since there is a LOS component with a higher signal strength compared to the other paths and many other reflected paths. The probability density function can be expressed as a casual Rice variable [21] [16]:

$$p(r) = \begin{cases} \frac{r}{\sigma^2} \exp\left(-\frac{r^2+r_s^2}{2\sigma^2}\right) I_0\left(\frac{r r_s}{\sigma^2}\right), & 0 \leq r \leq \infty, \\ 0, & elsewhere, \end{cases} \tag{1.11}$$

where r_s^2 is the direct component signal strength, σ^2 is the power of the other components and I_0 is the Bessel function of order zero and first type.

Moreover, it is important to describe how the direct component is dominating on the others; this is represented by the K factor, the ratio between the direct component and the reflected components signal strength:

$$K = \frac{r_s}{\sigma^2} \tag{1.12}$$

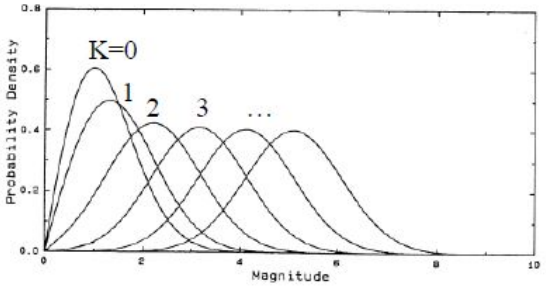

Figure 1.7: Signal strength distributions for different values of K

It is also important to show that for K=0 the Rice distribution becomes the Rayleigh distribution.

1.4.2 Doppler Effects

Another important effect of big interest is called *doppler effect*. It is characterized and defined using different parameters: Doppler spread and coherence time, doppler frequency and coherence bandwidth.

The *doppler frequency* consists in a frequency shift (*i.e.* a shift of the wavelength) of all the components at the receiver due to its relative motion at a certain velocity v with respect to the transmitter. The frequency variation of the received signal can be expressed as [21]:

$$\Delta f = \frac{v}{\lambda} \cos \vartheta \tag{1.13}$$

where v is the velocity of the receiver, λ is the signal wavelength and ϑ is the angle of arrival of the signal with respect to the ground in direction of the motion.

It can be observed that in the case of a receiver moving toward the transmitter the time of propagation is decreasing and the frequency is increasing. In the opposite case, instead, the receiver is getting away from the transmitter and so, the propagation time is increasing (*i.e.* a delay is present in the

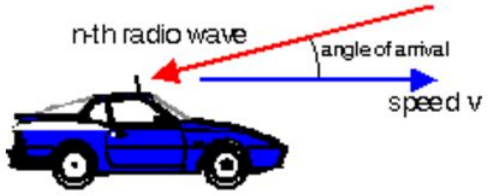

Figure 1.8: The doppler effect

received signal) and the frequency is decreasing. The *doppler shift* can be expressed as:

$$f_d = f_c \frac{v}{c} \cos \vartheta \tag{1.14}$$

where f_c represents the signal carrier frequency and c is the speed of light. On the basis of the *doppler shift* also the *doppler spread* can be defined as the variation of the spectrum of the received signal around the carrier frequency f_c of a value equal to the doppler shift f_d; it will refer to a total bandwidth $B = 2f_d$ between the frequencies $f_c - f_d$ and $f_c + f_d$.

Moreover, the *coherence time* T_c is used to give a better description of the time interval where the channel remains almost constant and quasi-static. It is proportional to the inverse of the maximum doppler shift $f_{d,max}$; it means that in that period of time the channel response is not significantly changing. It can be expressed as:

$$T_c = \sqrt{\frac{9}{16\pi f_{d,max}}} \tag{1.15}$$

It is useful to define also the coherence bandwidth that states which is the bandwidth within which the signal can be considered not distorted from the channel. It can be expressed as:

$$B_c = \frac{k}{\tau_{max}} \tag{1.16}$$

where k is a constant (usually equal to $\frac{1}{10}$ or $\frac{1}{5}$) and τ_{max} is the maximum delay of the reflected paths with respect to the direct component [16].

Chapter 2

Device-to-Device Communications

2.1 Introduction to Device-to-Device

In this chapter, a complete analysis and a full description of the Device-to-Device (D2D) communication, added to LTE in 3GPP Release 12 (LTE-A), is given. D2D is a specific type of communication that "refers to a radio technology that enables devices to communicate directly with each other when they are in close proximity, without routing the data paths through a network infrastructure" [37]. Direct communication between nearby mobile devices will improve spectrum utilization, overall throughput, and energy consumption, offering high data rates and low end-to-end delay, while enabling new peer-to-peer and location-based application and services (Proximity services, largely driven by the social networking applications, *i.e.* ability to discover users and/or services that are in proximity, called *ProSe*) [40]. Basically, D2D offers direct communications between users, bypassing the base station (eNB) and the core networks, without using the cellular network infrastructure; this kind of communications is being fulfilled, firstly, for public *safety radio systems*, largely used in case of emergency when cellular networks are not available or fail, such as in the case of large-scale disasters (*i.e.* in case the eNB

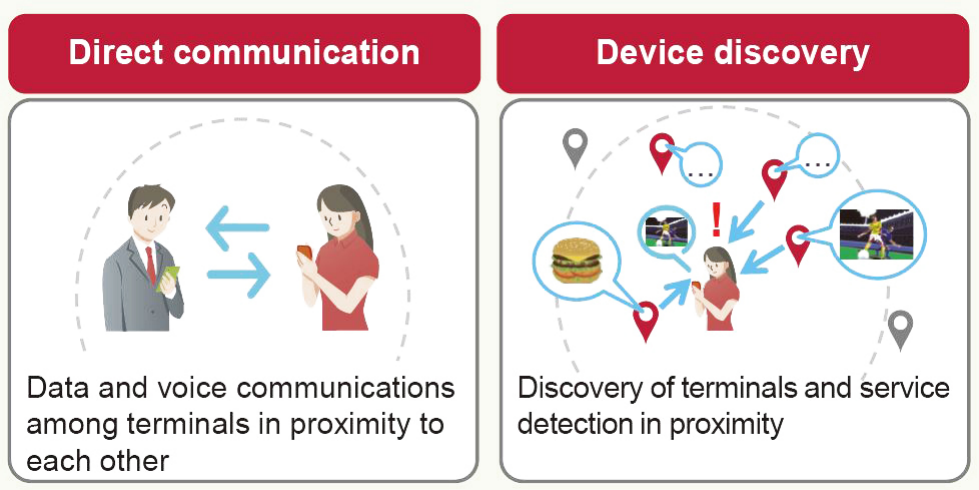

Figure 2.1: D2D communication types [37]

could be not operational) or in a particular area where the eNB is not able to cover, in addition to cellular systems to reduce operational costs, ensure interoperability by standardized specifications and provide broadband communications [37]. D2D communications are «typically deployed using underlaid transmission links which reuse existing licensed spectrum resources» [30]. Two main types of communication can be identified: direct communication, where data and voice communications take place between users that are in proximity to each other and device discovery, that is referred to the discovery of services and other UEs in proximity for *ProSe*.

2.2 Communication Scenarios

Three coverage scenarios can be identified in the case of a D2D communication [25], as shown in Figure 2.2:

- *In coverage* scenario: all the resources used for communicating are controlled by the network (*i.e.* interferences with cellular traffic is avoided), that may assign specific resources to a transmitting UE or a pool of resources the UE selects from.

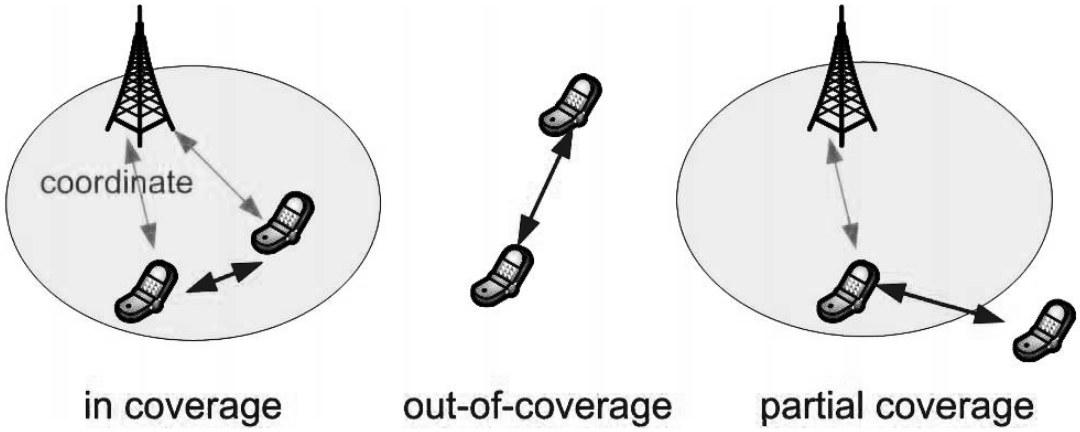

Figure 2.2: Coverage scenarios for D2D communications

- *Out-of-coverage* scenario: the resources that a UE has to use in this case are preconfigured either in the mobile device or in the USIM [4]. Out-of-coverage, here, means that the UE could possibly be in the coverage of an eNB for cellular traffic (on a different frequency) but out-of-coverage on the frequency that is being used for D2D communication.

- *Partial coverage* scenario: the UE that is out of coverage uses a preconfigured resources while the in-coverage UE gets the resources from the base station.

2.3 Network Infrastructure

For describing the network infrastructure, Figure 2.3 has to be considered. A terminal UE in the coverage area interacts with ProSe Function, which is a logical function in Evolved Packet Core (EPC) for D2D, with the aim of authenticating the D2D terminals, using Home Subscriber Server (HSS), while SLP (Secure User Plane Location) "is used to distribute suitable communications settings according to the terminal locations" [37]. From a UE point of view, the one-to-many communication interface PC5 between two UEs and

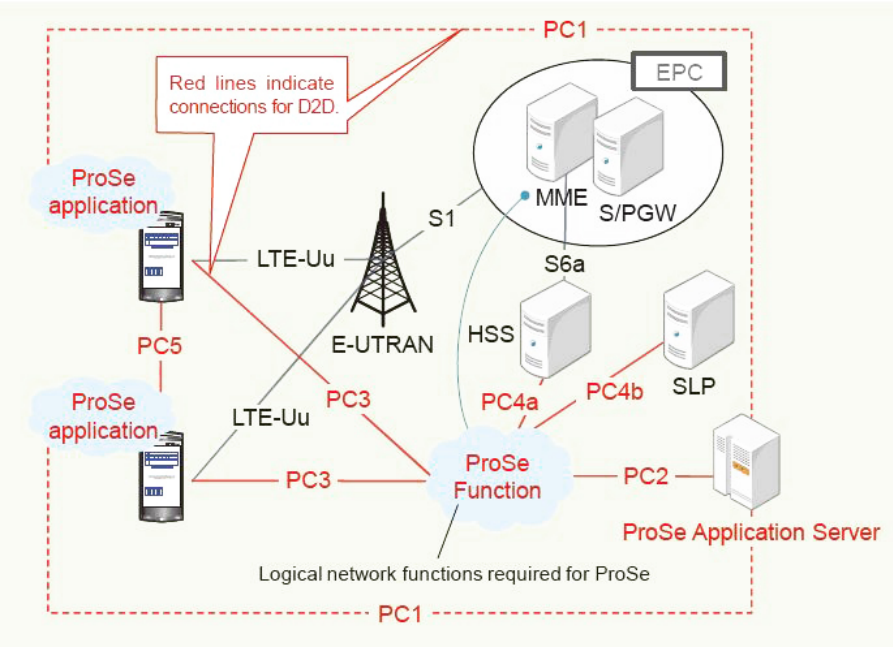

Figure 2.3: D2D Architecture

the PC3 interface between the ProSe function and the UE are identified; using the latter interface, a UE can contact the ProSe function, establishing a RRC connection with the network (RRC_CONNECTED state) knowing its IP address, that has been either preconfigured or got via DNS look-up. In this way, the UE receives information for network related actions, including service authorization and PLMN (*i.e.* "a network that is established and operated by an administration or by a recognized operating agency (ROA) for the specific purpose of providing land mobile telecommunications services to the public» [23]) specific information, exchanging IP messages (*i.e.* HTTP Request and Response messages) [25]. In the case of Public land mobile network, the ProSe Function sends security parameters, group IDs (that «identify the PDCP / RLC pair to be used in the receiving UE" [25]), group IP addresses («including the indication whether the UE shall use IPv4 or IPv6 for the group» [25]) and Radio resources parameters for the usage in out-of-coverage scenarios.

2.4 Protocol Stack

For D2D communication the same protocol stack of LTE-A is used (Figure 2.4). At physical layer the PC5 interface is used (as previously explained). At MAC layer, messages containing ProSe UE ID (24 bits, used as Source field in each MAC PDU) and ProSe Layer-2 Group ID (24 bits to identify the group) are sent to identify the transmitting UE and the transmission group. They can be preconfigured in the UE or provided by the Network and, together with logical channel ID, they identify the PDCP/RLC pair to be used in the receiving UE. For each transmitting UE and each logical channel the receiving UE has to keep this pair (this operation is done at the first MAC PDU reception). MAC layer supports blind retransmission of messages without feedback (HARQ). "In contrast to current LTE-A systems, where the radio bearer is terminated at the UE and the eNB, the endpoints of the direct path communication are at the two UEs. Hence, the RRC configuration provided by the eNB to both UEs should be compatible with each other. Radio Link monitoring, measurement, and handover procedures also need to be altered to accommodate direct path aspects". "To maintain the best connectivity, the handover from D2D network to cellular network shall take place when the cellular connection attains more throughput and lower energy consumption than that of D2D" [36].

2.5 Communication between eNB and UE

"SIBs (system information block) messages carry relevant information for the UE, which helps UE to access a cell, perform cell re-selection, information related to INTRA-frequency, INTER-frequency and INTER-RAT cell selections" [6]. An eNB indicates that it supports a sidelink D2D communication with a System Information Block signal called SIB18, that is broadcasted on

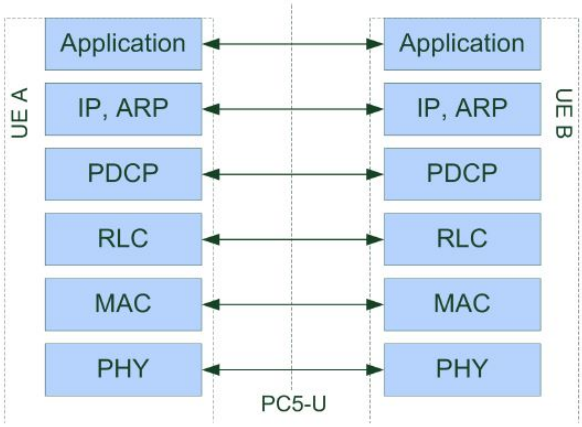

Figure 2.4: Protocol stack

BCCH. It contains [25]:

- a list of RPs (resource pools) called *commRxPool* (up to 16 RPs) where the UE is allowed to receive a sidelink transmission (it may include RP from dedicated resource assignment, and UE out-of-coverage). Dedicated assignment is done only for Transmission pools
- 4 RPs are present in *TxPoolNormalCommon* for transmission in RRC_IDLE state
- 4 RPs in *TxPoolExceptional* for transmission when a transition between RRC_IDLE and RRC_CONNECTED occurs
- *commSyncConfigList* contains the necessary information for synchronization between UEs which are not in coverage of the same cell (in this case additional synchronization signals are needed, called SLSS and MIB-SL)

When a UE is in RRC_CONNECTED state and it needs to request/release resources for direct discovery from/to the eNB, it does not use the resources available in the broadcast message SIB18 but it requests dedicated resources for transmitting (it means that it has data to transmit in a sidelink) to the base station using *SidelinkUEInformation* message that contains [26]:

- the frequency that the UE wants to use to receive/transmit
- a list of 16 destination IDs (this message can be sent to other eNBs that didn't broadcast SIB18 so that they can be advised in advance)
- *discRxInterest* (set to true or false) to indicate its interest in reception of sidelink discovery messages
- *discTxResourceReq* indicating the number of resources required for sidelink (an integer from 1 to 63)

The eNB can provide either a list of 4 RPs (and the UE can then select randomly the resources from the assigned ones, mode_2) or scheduled resources (UE knows exactly where to transmit thanks to DCI (downlink control information) message, mode_1) knowing time and frequency resources to transmit the SCI (sidelink control information), containing the information needed to the rx UE to demodulate the received data.

2.6 Sidelink Transmission

Usually, in cellular traffic over U_u, a UE and its eNB can communicate and exchange signaling and data, using the uplink and downlink links; in the case of D2D communication, a new type of link called sidelink (SL) has been introduced, corresponding to the PC5 interface described in the network infrastructure section. The resources assigned to the SL are taken from the subframes on the UL (because UL subframes are usually less occupied than the subframes than the DL). Moreover, the sidelinks represent the logical, transport and phisical channels used in the air-interface to realize a ProSe application. [25]. The information regarding SL communication are broadcasted by the eNB using SIB18 messages, that are indicating the SL support by means

of many parameters inside (like PLMN identities of neighboring cells used by UE in IDLE/CONNECTED MODE); by receiving the SIB18 the UE knows that eNB supports SL Transmission. This is important because the eNB can avoid scheduling cellular traffic to the UE since it cannot receive cellular traffic and sidelinks transmission simultaneously in the same subframe of the same carrier.

Two SL logical channels are present: STCH (sidelink traffic channel) and SBCCH (sidelink broadcast control channel). The first one is a point-to-multipoint channel used for transmitting data, carrying user information from the ProSe application; it is connected to the transport channel called SL-SCH (sidelink shared channel) that in turn interfaces the PSSCH (physical sidelink shared channel). The second one, instead, is used for carrying information either used for the out-of-coverage case of partial coverage scenarios or for synchronizing UEs in different cells; it is connected to the transport channel called SL-BCH (sidelink broadcast channel) that in turn interfaces the PSBCH (physical sidelink broadcast channel) [25].

2.7 Resource Pools (RP)

A resource pool is "a set of resources assigned to the sidelink operation. It consists of the subframes and the resource blocks within" [25] and "it is configured semi-statically by layer 3 messaging using the layer 3 SL-CommResourcePool RRC message. The layer 1 physical resources (subframes and resource blocks) associated with the pool are partitioned into a sequence of repeating 'hyper-frames' known as PSCCH periods (called SC, sidelink control period). Within a PSCCH period there are separate subframe pools and resource block pools for control (PSCCH) and data (PSSCH). The PSCCH subframes always precede those for PSSCH transmission" [1]. Figure 2.5 shows a RP for SL communi-

cation (the blue boxes inside the bitmap are the subframes used for RP); the subframes bitmap is divided into control and data region and the whole pattern will be repeated after a SC period (Sidelink Control Period). Inside each RP subframe the resources used for SL are divided into two bands, having a width of PRB-Num resource blocks (RB), marked by two flags called PRB-Start and PRB-End that are determining which resource blocks are reserved for transmission in a subframe dedicated to D2D. "Cellular communication takes place in FDD DL while D2D takes place in UL band in FDD and UL subframe in TDD" [36]. Using such a subframe organization, it is possible to have more RPs inside the same subframe and using the remaining for cellular communications. Two types of RPs can be identified: Rx RPs (reception resource pools) and Tx RPs (transmission resource pools) and they can either preconfigured (in case of out-of-coverage) or communicated by the eNB (in-coverage case). Moreover, in order to permit any type of communication, for each Tx RP there must be at least one Rx RP (more often there are many Rx RP for each Tx RP). In the end, two main modes of resource assignment are present; in *Mode_1* the base station eNB indicates the resources to be used via DCI format messages sent to the transmitting UE, in *Mode_2* the UE self-selects a RP and the resources there assigned according to rules aimed at minimizing the collision risk [25].

2.8 Synchronization

The *synchronization* can be performed in two different cases: inside and outside eNB coverage area. In the partial case, in particular, additional synchronization signals are used, so that they can enable detection of the synchronization source ID, frequency and reception timing required by the terminals to start communicating. In order to demodulate data, the transmitter UE

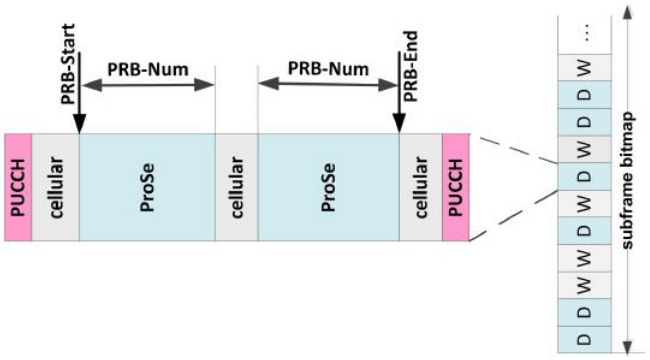

Figure 2.5: Resource Pool for Sidelink Communication. The subframes to be used for RP are the blue ones.

and receiver UE must be synchronized each other [36]. There are two types of synchronization signals, as explained in [25]:

- *Sidelink Synchronization Signals* (SLSS), for synchronization in time and frequency. SLSS can be primarily sidelink synchronization signals (PSSS) and secondary sidelink synchronization signals (SSSS), both occupying 62 Resource Elements in frequency and two adjacent SC-FDMA symbols in time, sent at 40 ms intervals. A SLSS ID is attached to the synchronization signals (respectively in a range from 0 to 167 if the UE is in coverage or is receiving synchronization from an UE in coverage and from 168 to 335 if the UE is out-of-coverage) so that the receiving UE can know whether the sender is in close connection to a eNB detecting it; the SLSS-ID is used as measurement parameter, using the sidelink reference signal received power (S-RSRP) and organizing them with priorities based on signals strength, if it is in-coverage or not. The rx UE will choose the UE that has sent the signal with the highest RSRP.

- *Master Information Block Sidelink* (MIB-SL) are transmitted over the SBCCH providing additional information. It contains the parameter *sl-bandwidth*, the *inCoverage* parameter (indicating if the sender is in coverage or not) and *directFrameNumber* and *directSubFrameNumber* in-

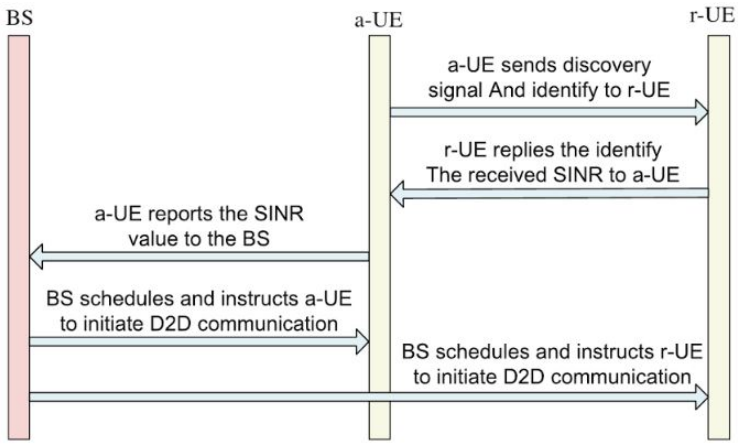

Figure 2.6: The loosely controlled discovery procedure

dicating the system frame number (SFN) and number of subframe to be used.

The other configurations, such as system bandwidth, frame number, UL/DL TDD subframe, are transferred through physical sidelink broadcast control channel (PSBCH), as well as PSSS/SSSS [37]. Of particular importance is the parameter called rxParametersNCell, responsible of making the UE know that it has to synchronize to the sender; in fact, if this parameter is included, the UE knows that either the associated tx resource pool is not synchronized to the sender or it is on a neighboring cell from a UE out-of-coverage.

2.9 Device Discovery

D2D discovery enables UEs to use the LTE air interface to identify other users that are in proximity. Two categories can be identified: restricted discovery and open discovery, in terms of whether permission is needed or not [40] (called *respectively EPC level discovery* and a *direct discovery*).

The first one regards the notifications sent to the terminals «about other terminals detected in the vicinity based on user interest information and UE location information registered by terminals in ProSe function» [37]. The second

one, instead, regards the case of discovering devices sending signals (*discovery messages*) directly from UE using PSDCH channel (physical downlink shared channel) periodically in the ProSe discovery cycle (from 320 ms of duration to 10.24 s). UEs will transmit discovery signals that may be detected by other devices, including its identity and other application-related information; the amount of information inside the discovery messages determines the required amount of radio resources [37]. It is possible to identify two types of device-discovery: *a priori* and *a posteriori*. In the first one the network and/or the devices detects D2D candidates for a communication session; it can be in *fully controlled mode* where "the announcing UE first registers to the network, and the receiving UE willing to engage in D2D communications sends a request to the network" (request messages) containing other information (such as an own identity, a buddy list, or offered/required services) or in *loosely controlled mode* in which "the network does not actively participate in the discovery process other than assigning beacon resources to the devices (see Figure 2.6). Such beacon assignments are broadcasted in the coverage area of the cell so that the announcing UE (transmitting a beacon) as well as the receiving UE (detecting beacons) can readily find one another". In the second one, instead, "the network (e.g., an eNB) realizes that two communicating devices are in proximity to each other and thereby they are D2D candidates when the communication session is already ongoing (in cellular mode) between the UEs"; "the UEs agree on a token that is unique to the already ongoing communication session. Once the token is established, the UEs register the token at the serving eNB that can easily recognize the two UEs as D2D candidates". [36]

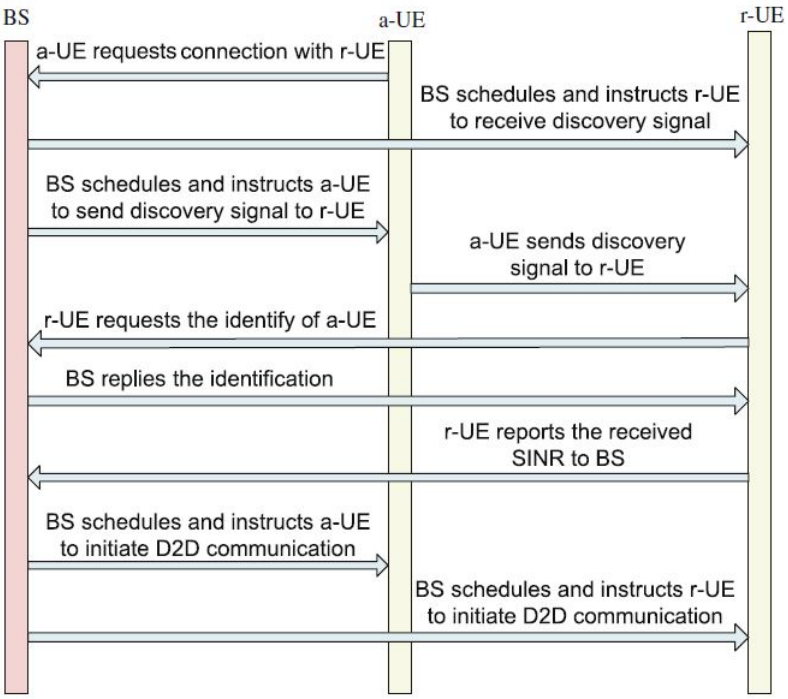

Figure 2.7: The fully controlled discovery procedure

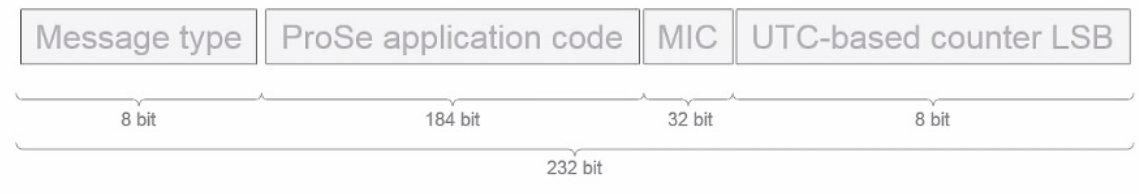

Figure 2.8: a D2D Discovery Message

2.10 Direct Communication

It is the communication between two UE devices in proximity using LTE air interface to set up a direct link without routing via eNB and possibly core network [40]. A direct UE to multiple UE communication (group communication) is possible without data transmission on the uplink or downlink. This is allowed for public safety applications only and supports one or more UEs being out of coverage (network and/or frequency) [1].“The direct data communication physical channel is expected to have a narrowband format and relatively low spectral efficiency in order to reach very large coverage, taking into account the limited antenna directivity and transmit power of devices and the challenging link budget” [36]. In direct communication two channels are used: PSCCH (physical control channel) and PSSCH (physical shared channel) both defined with ProSe communication cycle of 40ms. The first one, is a control channel that notifies scheduling for data sent with using the second shared channel (PSSCH) for direct communication. Moreover, it does not support a feedback channel function (*i.e.* ACK and NACK are kept in the upper layers) [37]. Nevertheless, scheduling and resources allocation are very important in direct communications; “The main challenge is preserving cellular traffic QoS from potentially harmful interference coming from out-of-coverage devices performing autonomous resource selection and power control” [36].

2.11 Benefits of D2D Communications

Direct communications between devices can provide several benefits to users in various applications where the devices are in close proximity, as said in [32]:

- *Data rates*: devices may be remote from cellular infrastructure and may

therefore not be able to support high data rate transmission that may be required

- *Reliable communications*: LTE Device-to-Device can be used for local communication between devices to provide high reliability especially if the LTE network has failed for a reason - even as a result of the disaster.

- *Instant communications*: as the D2D communications does not rely on the network infrastructure, the devices could be used for instant communications between a set of devices in the same way that walkie-talkies are used. This is particularly applicable to the communications that may be used by the emergency services.

- *Use of licensed spectrum*: unlike other device-to-device systems including Wi-Fi, Bluetooth, etc., LTE would use licensed spectrum and this would enable the frequencies to be used to be less subject to interference, thereby allowing more reliable communications.

- *Interference reduction*: by not having to communicate directly with a base station, fewer links are required (*i.e.* essentially only between devices) and this has an impact on the amount of data being transmitted within a given spectrum allocation. This reduces the overall level of interference.

- *Power saving*: using D2D communication provides energy saving for a variety of reasons. One major area is that if the two devices are in close proximity then lower transmission power levels are required.

2.12 Device-to-Device vs Mobile Ad Hoc Networks (MANETs)

As explained in [36, 40] there are two most important differences between D2D and Ad Hoc Networks communications. First, "D2D can typically rely on assistance from the network infrastructure (*i.e.* eNBs) for control functions like synchronization, session setup, resource allocation, routing, and other overhead-consuming functions that are extremely costly in a MANET" [40]. Moreover, "D2D networking mainly consists of local, opportunistic, and single-hop communication, whereas multihop routing is typically needed in a MANET, and long hops may be unavoidable, which hurts network performance"; although, "in the public safety context, D2D must function even without eNB support, so it is more like a MANET".

2.13 Challenges and Issues of D2D

If from one side D2D might seem to be a great improvement and innovation in cellular communications, on the other one it has some possible issues that have to be taken into account. First, the biggest issue is related to the share of radio resources with the cellular network uplink; it can happen that some unexpected high-level interference arises in adjacent frequency resources, mainly on the uplink. In fact, a base station eNB might have problems in managing D2D communications outside its coverage area and communications with UE inside the coverage area at the same time (*i.e.* orthogonal multiplexing of radio resources both for cellular and D2D communications). Another big issue, is the fact that a UE cannot transmit and receive D2D messages simultaneously. There are many solutions that can be implemented in this sense. The first one is to choose a precise *resource assignment* method in which ei-

ther the UE chooses autonomously the transmission resources (possible both inside and outside the coverage area of the base station) or the eNB assigns the resources to the UE. Another possible solution can be the repetition of the transmission and time frequency hopping using the PSCCH, PSDCH and PSSCH channels; this would reduce the probability of having conflicts between different transmissions [37].

Chapter 3

Coverage, Capacity, Interference Results and Power Consumption Analysis

3.1 Introduction

As already said, the field of aerial base station (ABS) is growing fast and the activities connected to the use of drones and UAV in telecommunication area are becoming wider. There are many projects with the aim of offering some feasibility studies or researches that have tried to give a more accurate analysis and description of the possible capabilities that an ABS could have [29] [38]; an important project that deal with hybrid Aerial-Terrestrial Communication for public communications and capacity enhancement during temporary events is called ABSOLUTE [11]. In this direction, the aim of this study is to offer some important and new results regarding the use of ABS; in particular, this chapter contains a complete analysis of the coverage that an ABS can offer, taking into account three different possible propagation scenarios (suburban, urban and urban high rise) with respect to the height of ABS. Nevertheless, starting

from this the optimal ABS height is identified (*i.e.* the one that maximize the coverage percentage) and a complete power consumption analysis for the ABS is done, taking into account both the transmitted power and the power needed to hover and fly. In the end, the effect of interference from the first tier of six adjacent cells in analyzed, offering signal-to-noise ratio and signal-to-interference plus noise ratio calculation.

3.2 ITU-R Procedure

In the following, the complete ITU-R procedure for building up the simulation scenarios (*i.e.* calculating spacing and width of the buildings) is given, as explained at [10].

"If it is assumed that, on average, buildings are evenly spaced, the number of buildings lying between two points can be estimated. The probability that a LOS ray exists is:

$$P(LoS) = \prod_{b-1}^{b_r} P(building\_height < h_{LoS}) \tag{3.1}$$

where *br* is the number of buildings crossed. For this simple model, three parameters are required:

– α: the ratio of land area covered by buildings to total land area (dimensionless);

– β: the mean number of buildings per unit area (buildings/km2);

– γ: a variable determining the building height distribution."

"For suburban to high-rise locations α will range from 0.1 to 0.8 and β from 750 to 100 respectively. The Rayleigh probability distribution P(h) of the height h defines the parameter γ:

$$P(h) = \frac{\exp(-\frac{h^2}{2\gamma^2})h}{\gamma^2} \tag{3.2}$$

Given α, β and γ the LoS coverage is computed as follows: a ray of length 1 km would pass over $\sqrt{\beta}$ buildings if they were arranged on a regular grid. As only a fraction of land α is covered, the expected number of buildings passed per km is given by:

$$b_1 = \sqrt{\alpha\beta} \tag{3.3}$$

and so for a path of length $r_{rx}(km)$, the number of buildings is:

$$b_r = floor(r_{rx}b_1) \tag{3.4}$$

where the floor function is introduced to ensure that an integer number of terms are included in equation (3.1). The probability of presence of a LoS ray at each range r_{rx} is obtained as:

Step 1: Calculate the number of buildings b_r between Tx and Rx points using equation (3.4).

Step 2: Buildings are assumed to be evenly spaced between the Tx and Rx points, the building distances being given as:

$$d_i = (i + \frac{1}{2})\delta_r \quad i \in \{0, 1, ..., (b_r - 1)\} \tag{3.5}$$

where $\delta_r = \frac{r_{rx}}{b_r}$ is the building separation.

Step 3: At each d_i the heigth h_i of a building that would obstruct the LoS ray is given by substituting d_i into equation $h_{LoS} = h_{tx} - \frac{r_{LoS} - h_{rx}}{r_{rx}}$

Step 4: The probability Pi that a building is smaller than height hi is given by:

$$P_i = \int_0^{h_i} P(h)dh = 1 - \exp\left(-\frac{h_i^2}{2\gamma^2}\right) \tag{3.6}$$

Step 5: The probability P_{LOS_i} that there is a LoS ray at position d_i is given by:

$$P_{LoS} = \prod_{j=0}^{i} P_j \quad j \in \{0, ...1\} \tag{3.7}$$

Step 6: The cumulative coverage is obtained weighting each P_{LoS_i} with weights W_i dependent on the distance from the transmitter. It accounts for the number of buildings in an annulus being greater at larger distance.

$$W_i = 2i + 1 \tag{3.8}$$

Step 7: Summing the building weighted probabilities and normalizing by the cumulative annulus area multiplied by building density gives the required coverage for a cell with radius r_{rx}":

$$CP_{r_{rx}} = \frac{\sum_{i=0}^{b_r-1} P_{LoS,i} W_i}{b_r^2} \tag{3.9}$$

3.3 Simulations Setup

In order to perform simulations, three different environments have been considered: suburban, urban and urban high rise, as shown in Fig 3.1, 3.2 and 3.3. These environments have been created using a Computer-Aided-Design software, called 3ds Max from Autodesk [2], based on ITU-R parameters found using the ITU-R procedure shown above (*i.e.* the number of buildings, the spacing between buildings and the width of each building of the scenario), as indicated in Table 3.1.

Scenario	Number of buildings	Spacing [m]	Width [m]
Suburban	750	24.97	11.54
Urban	500	20.22	24.50
Urban High Rise	300	16.91	40.825

Table 3.1: ITU-R calculated values of number of buildings, distance between buildings and width of each building for different propagation scenarios

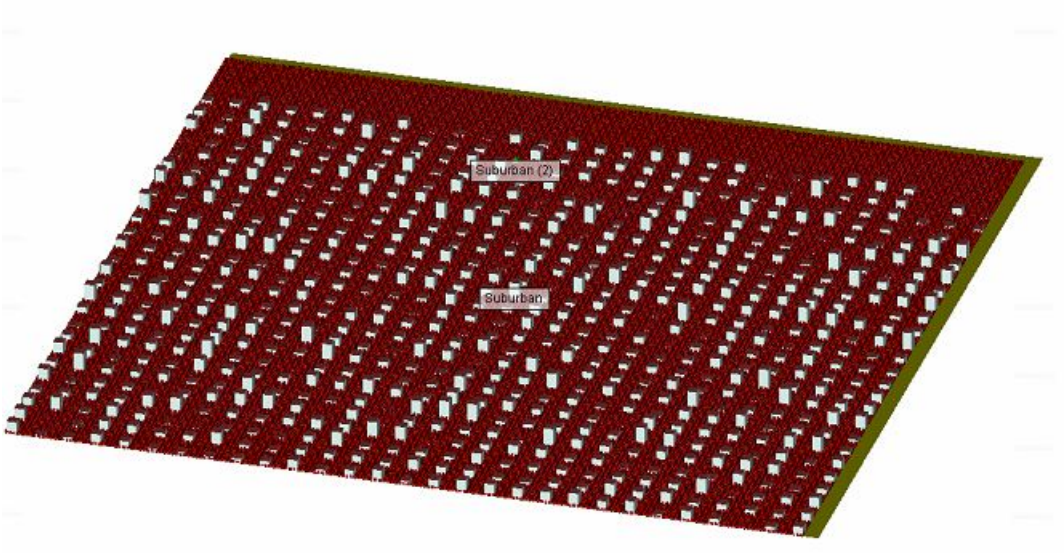

Figure 3.1: Suburban maps built in 3ds Max following ITU-R specifications used for simulations in Wireless Insite

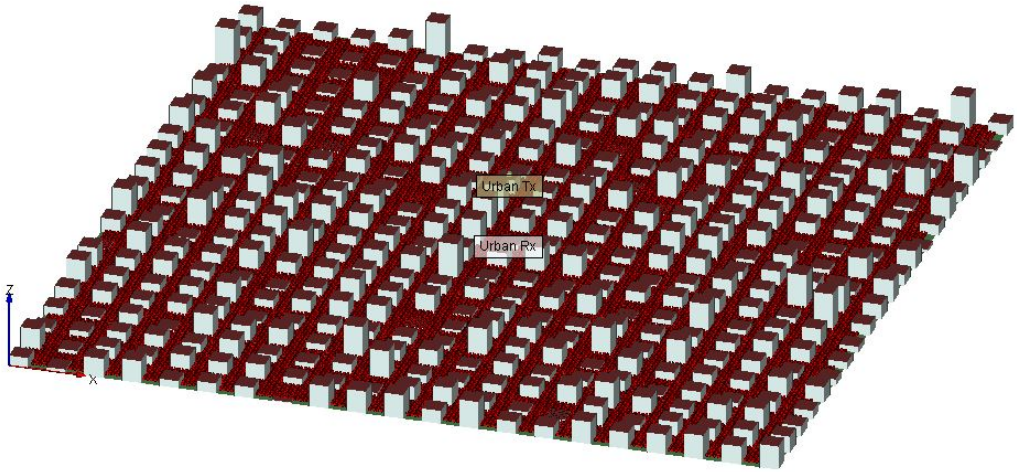

Figure 3.2: Urban maps built in 3ds Max following ITU-R specifications used for simulations in Wireless Insite

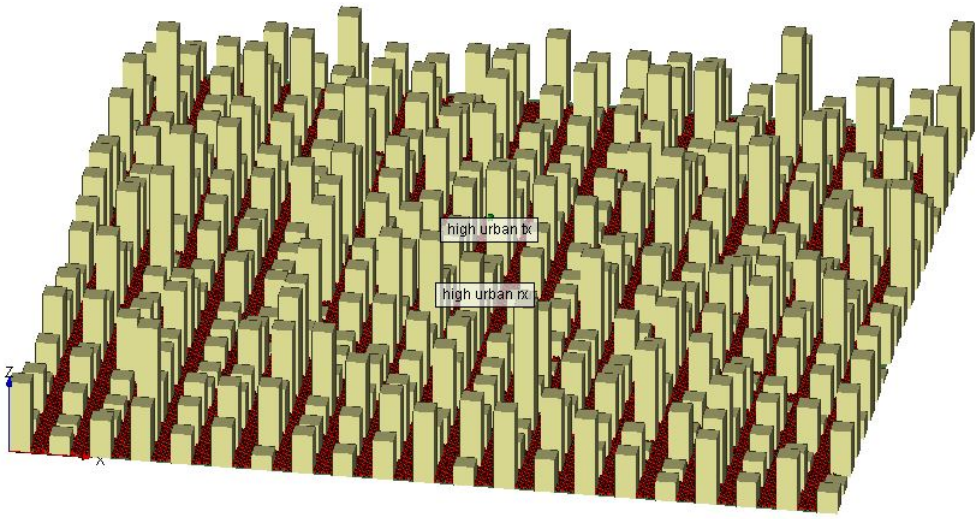

Figure 3.3: Urban high rise maps built in 3ds Max following ITU-R specifications used for simulations in Wireless Insite

The buildings are uniformly distributed over the environment with a height that follows a Rayleigh distribution. Creating the simulations scenario like that has permitted us to generalize of the environments, with the great benefit of approximating the results for any city in the world. The chosen environments size is $2000 \times 2000\ m^2$. However, to reduce sensitively the computation time, the simulations have been performed on a reduced $1000 \times 1000 m^2$snapshot area. In particular, two snapshots from each environment have been created to verify and improve the accuracy of the overall results. In each environment map 32.500 receivers (Rxs) (red dots on Fig 3.1, 3.2, 3.3) have been placed on the streets of the city, each one at 5m apart from the other and 2m above the ground. The transmitter (Tx) has been placed at center of the snapshot, approximately. Both the receivers and transmitter have been equipped with isotropic antennas and the noise figure has been set at 3dB in the simulator.

Moreover, 120 different simulations, one for each snapshot, scenario and each ABS height (from 100 to 2000 m with an interval step of 100 m) have performed in order to maintain the sensitivity of the results. For the simulation, a sinusoid waveform has been transmitted at carrier frequency $f_0 = 2.4GHz$

and a signal bandwidth $B = 20MHz$, keeping the standard sea level atmospheric conditions. For computing the simulations a ray tracing software called Wireless InSite 3.0.1 from Remcom [9] has been used, whose accuracy with comparison to practically measured results is well defined in [27].

3.4 Air-to-Ground Communication Channel

As given in [12, 33], the air-to-ground (A2G) channel is well-defined as probabilistic LOS and NLOS models and Close-In reference distance model. The PL due to large scale fading and shadow fading in dB is defined by:

$$PL_{LOS}(d)[dB] = 20\log\left(\frac{4\pi d_0}{\lambda}\right) + 10n_{LOS}\log(d) + X_{\sigma,LOS}; \tag{3.10}$$

$$PL_{NLOS}(d)[dB] = 20\log\left(\frac{4\pi d_0}{\lambda}\right) + 10n_{NLOS}\log(d) + X_{\sigma,NLOS}; \tag{3.11}$$

for LOS and NLOS, respectively, where λ is the wavelength in meters, η is the PLE, d is the link distance in meters, d_0 is the reference distance, here assumed $d_0 = 1m$ and X_σ is the lognormal random variable (Gaussian in dB) with standard deviation σ that models the large-scale shadowing. The total path loss is given by:

$$PL(d)[dB] = P_{LOS} \cdot PL_{LOS}(d) + (1 - P_{LOS}) \cdot PL_{NLOS}(d); \tag{3.12}$$

where P_{LOS} is the probability to have a LOS link [12]. Also, for our simulations we obtain the Path Loss Exponent (PLE) from the simulation results [33].

For defining the small scale fading characteristics for our simulations, the

channel power gain is assumed to follow a Rician distribution since in the in A2G channel there is a dominant LOS component. However, this also depends on the chosen environment, as seen from the results that will be discussed in the following.

3.5 Optimal Height of an Aerial Base Station for Maximum Coverage

Low Altitudes Platforms (LAPs) are quasi-stationary aerial bodies, such as rotor-crafts, balloons, helikites or drones etc.; it has been decided to consider the LAP as a drone because of easy maneuverability, reliability and better stability in wind conditions. In this chapter, for the coverage analysis, with respect to wireless communications, we consider the *coverage* to be defined as the portion of the cell in which the received power of GS (Ground Station) is above a given threshold, which is established by the mobile operator. Therefore, the following equation has been used to define the cell coverage [17]:

$$C = \frac{1}{A_c} \int_{A_C} r \cdot P(P_{rx}(r) \geq P_{min}) dr d\vartheta \tag{3.13}$$

where A_c is the cell area of radius R that has been chosen to be equal to 200 m, r is the distance of each receiver from the ABS and $P(P_{rx}(r) \geq P_{min})$ is the probability that the received power at distance r $P_{rx}(r)$ is greater than the threshold P_{min}. Moreover, for obtaining the coverage, a sectorization of the snapshot has been done on the basis of a 2°elevation angle between the ABS and GS (*i.e.* incrementing of 2° the elevation angle at each sector) as shown in Fig 3.4, for discretizing the coverage formula from the continuous case to the corresponding discretized one.

For each sector, then, the probability P was calculated from the simulated

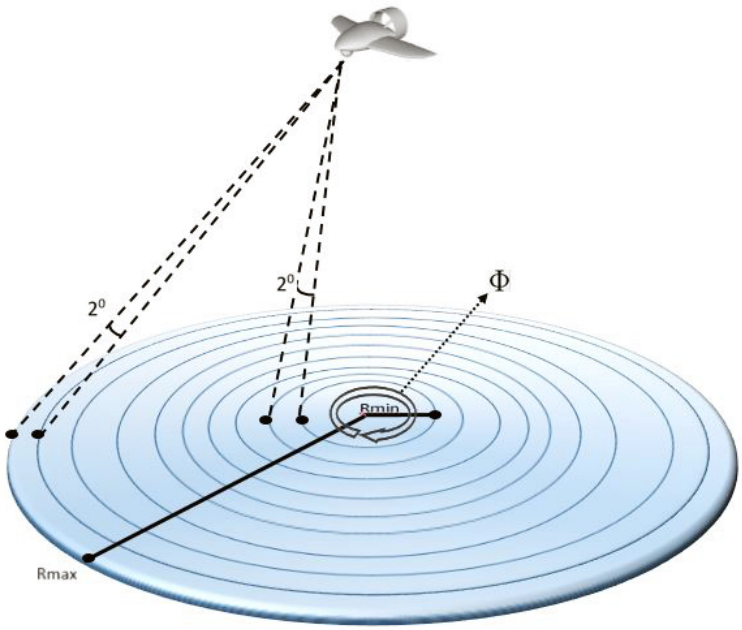

Figure 3.4: Coverage analysis from aerial base station with secotorization procedure

Scenario	Cell Area ($R = 200m$)	Buildings Area [m^2]	Final Cell Area [m^2]
Suburban	103,923.04	10,379.69	93,543.35
Urban	103,923.04	31,189.904	72,733.14
Urban H R	103,923.04	51,961.95	51,961.08

Table 3.2: Values of the cell area including and excluding the buildings inside each cell

data for the receivers (Rxs) within that sector and their distance from the transmitter (Tx); as already said, the cell area was taken to be hexagonal of radius $200mt$ (the area can be calculated using the formula $A = \frac{3\sqrt{3}R^2}{2}$), removing the total buildings area where no receivers are present, as shown in Table 3.2:

Having the Final Cell Area values A_c in m^2, the coverage calculations have been computed for both the snapshots of all the scenarios (suburban, urban and urban high rise) and all the heigth (from 100 to 2000 m) of the ABS, and the whole bunch of results has been plotted, as shown in Figure 3.5.

It can be seen that, as expected, the bigger value is obtained for the subur-

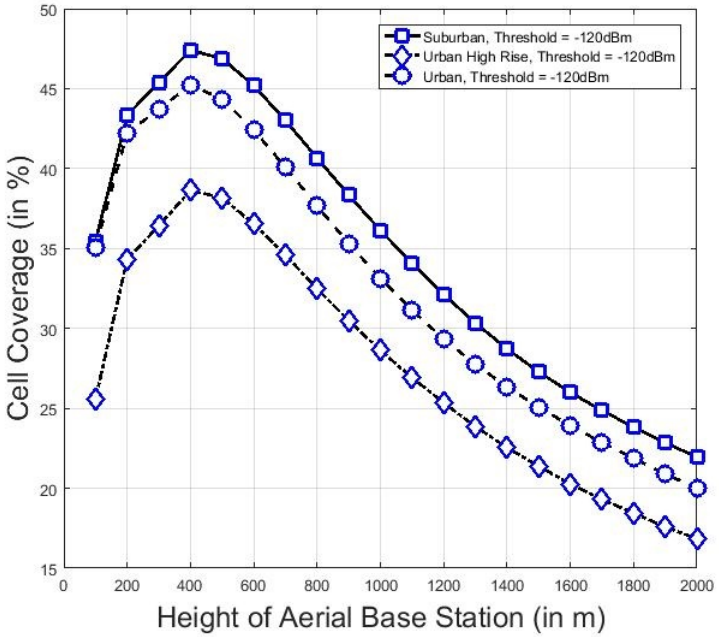

Figure 3.5: Coverage percentage results w.r.t. to the height of the ABS for all the scenarios and snapshots using -120 dBm as receiving threshold

ban environment with a peak of almost 47 % of cell coverage, followed then by the urban case with a maximum percentage of almost 45 % and last but not least the urban high rise case that has shown a value of coverage near 40 % in the point of maximum; as expected the cell coverage is higher for suburban environment than urban environments, due to Rayleigh fading where multi-path and scattering effects dominate leading to constructive and destructive addition of received power with their phase and delay and therefore leading to higher received power.

The same approach has been followed for other two cases, maintaining the same transmitted power P_{TX} equal to 18 dBm and changing the receiving threshold from -120 dBm to -100 dBm first and -80 dBm then, to see which are the results of coverage in these cases, as shown in Figure 3.6 and 3.7.

In this case, it can be observed that the behavior is changed as the threshold increases because of some propagation phenomena encountered. In fact,

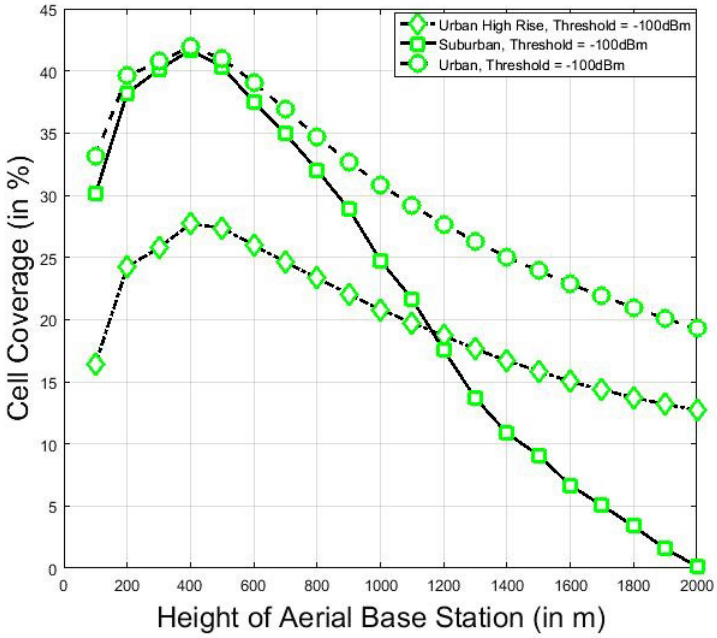

Figure 3.6: Coverage percentage results w.r.t. to the height of the ABS for all the scenarios and snapshots using -100 dBm as receiving threshold

in urban conditions, A2G channel experiences Rician fading due to the presence of LOS with a higher signal strength compared to the other paths and many other reflected paths; in suburban areas, instead, a Rayleigh fading is experienced due to the presence of reflected signals that are stronger than LOS component. Therefore, as received power threshold is increased, fading changes from Rayleigh to Rician in suburban environments and vice versa in urban; for this reason, a generalized approach is to use a Rician distribution where both LOS and NLOS paths are considered.

Nevertheless, the coverage is also changing and the values are mostly lower w.r.t. the previous threshold case; it can be stated that for suburban the higher value is decreased till 43 % almost, for the urban environment the coverage is decreasing till 42 % and for the urban high rise there is a more than 10% loss in the coverage with a maximum value of 28 % almost.

In the case of -80 dBm as receiving threshold the behavior is changing a

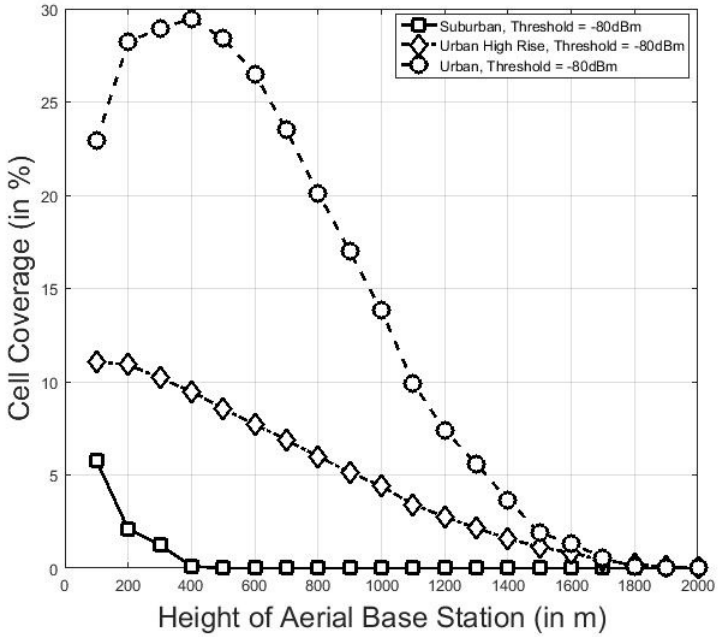

Figure 3.7: Coverage percentage results w.r.t. to the height of the ABS for all the scenarios and snapshots using -80 dBm as receiving threshold

lot w.r.t. the latter case and it can be seen that, if on one hand the coverage percentage value in the case of urban environment is decreasing but still maintaining a percentage around 30 % with a loss of 10 % almost w.r.t. the -100 dBm threshold case, on the other hand, in the case of suburban and urban high rise, the percentage of coverage is very low, going to zero in the case of suburban propagation; this conclusions are confirming the destroying effects of propagation phenomena previously explained.

The second part of our work, has been to characterize the height of the ABS w.r.t. the maximum coverage value. It can be seen that the value of maximum coverage percentage for all the scenarios is given for the same range of values of the height that, in this sense, will be the optimal height. The range of heights in which the coverage is maximize can be individuate as:

$$300m \leq h_{opt} \leq 400m \tag{3.14}$$

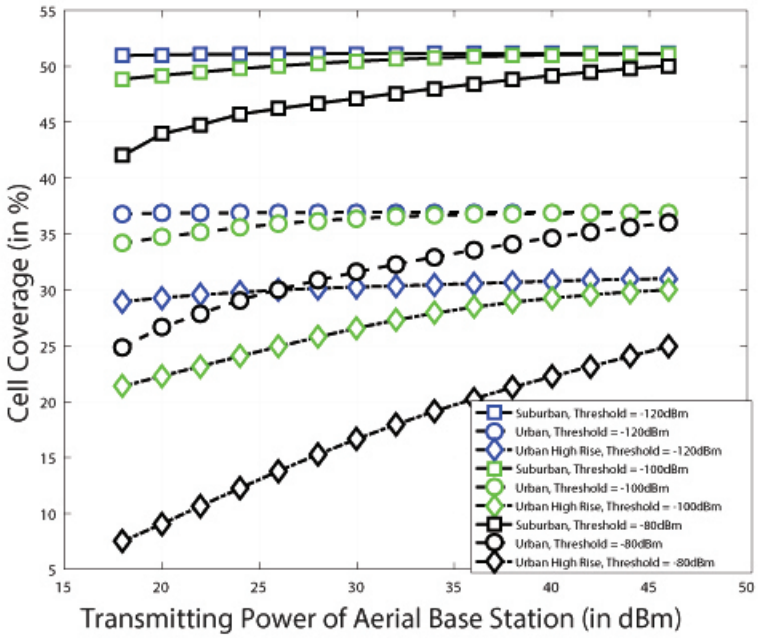

Figure 3.8: Coverage percentage results for an ABS at 320 m w.r.t. increasing transmitted power using -120, -100 and -80 dBm as receiving threshold

Because of this behavior, a new set of simulations has been done at a later stage to investigate how the coverage is increasing by increasing the transmitted power level from 18 dBm to 46 dBm (that is a common maximum LTE transmitted power level) using an interval step of 2 dBm between each simulation and the next one. For doing that, an optimal height $h_{opt} = 320.7526296$ m has been chosen for doing the new set of simulations. It has been found that the behavior, that can be seen in Figure 3.8, is linear as expected.

More in detail, Figure 3.8 shows that in the case of -120 dBm as threshold, an incrementing in the transmitted power brings a quasi-null increment in the coverage, that, in the best case, is moving of 2% from the initial value, becoming almost constant. This is because the Rxs receiving -120 dBm are already receiving the least value of received power to maintain the connectivity with the ABS and, therefore, the Rxs receiving less than -120 dBm are not present in the coverage area of the cell. Moreover, Figure 3.8 is showing a

good increment in the cell coverage in the case of -100 dBm of threshold, that is incrementing of almost 4-5% for both the suburban and urban environment, and even more (almost 10%) in the case of urban high rise. Finally, Figure 3.8 is showing the results in the case of a threshold set at -80 dBm; it can be seen that in this case the increment in coverage is very high, going from a 8% in the case of suburban, to a 10% in the case of urban communication, till almost 20% of increment in the case of urban high rise environment.

3.6 Capacity Analysis and Results

Channel capacity is the key parameter that defines the performance of a communication system. It is the upper bound limit on the rate at which information can be reliably transmitted over a wireless communication channel with arbitrarily low probability of error. For these computations, a flat fading channel with stationary and ergodic time-varying gain $g(i)$, with $g(i) \geq 0$, and Additive White Gaussian Noise (AWGN) $n(i)$ at each time i has been considered. Moreover, $g(i)$ has been considered an independent and identically distributed random process, distributed according to Rician probability density function in order to take into account small scale fading effects even if the majority of propagation loss is due to large scale fading. Capacity is defined as [21]:

$$C = B \cdot \log_2(1 + SNR) \tag{3.15}$$

where B is the signal bandwidth and SNR is the instantaneous Signal-to-Noise Ratio defined by:

$$SNR = \frac{S}{N} = \frac{P_{rx}}{N_0 B} = \frac{s_{g(i)}}{N_0 B} \tag{3.16}$$

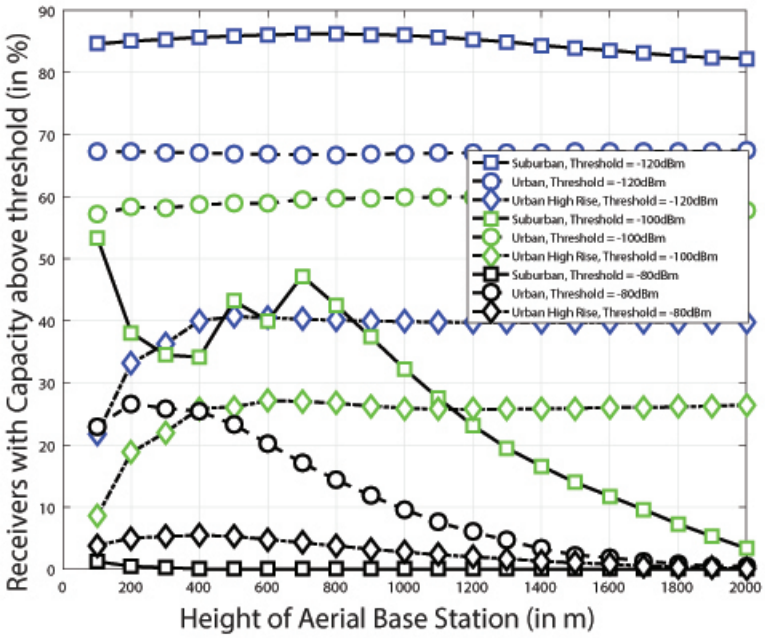

Figure 3.9: Capacity analysis from an ABS at 18 dBm of Tx power for different Rx thresholds

where $P_{rx} = s_{g(i)}$ is the i-th received power and N_0 is the spectral density of the noise.

Figure 3.9 is showing the results that have been computed in terms of percentage of receivers with capacity (*i.e.* SNR) above the threshold, that has been set at -120, -100 and -80 dBm, with respect to the ABS height.

Fig 3.10, instead, shows the percentage of receivers with capacity above the threshold, considering the cases of minimum and maximum RSSI for the simulations, carried at an optimal altitude of 320 m. It can be seen that the percentage of receivers with capacity above the threshold increases increasing the transmitted power as expected, since, the SNR increases linearly with the transmitted power and the capacity increases logarithmically with the SNR. Similarly, as it has been previously observed, the percentage is higher for simulation with -120 dBm threshold than -80 dBm; also, the behavior of capacity percentage is similar at both thresholds unlike the variation due to

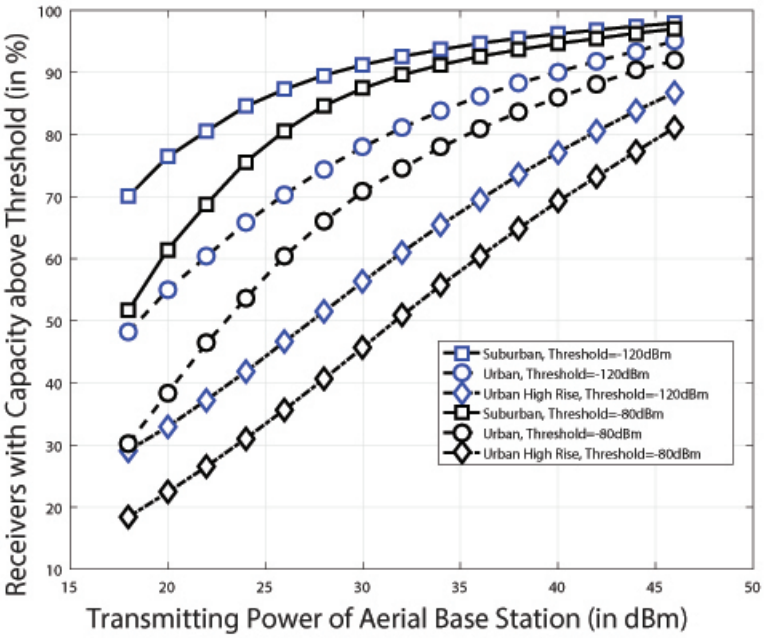

Figure 3.10: Coverage analysis from an ABS at 320 m of height with varying Tx power for different Rx thresholds

Tx height, with suburban having the maximum percent than urban and urban high rise because, again, Rayleigh fading effects in suburban and Rician in urban environments are encountered.

3.7 Interference Analysis and Results

Another important aspect that has been analyzed in this thesis is the impact of inter-cell interference coming from the adjacent cells ABSs. This effect impacts the received power of a GS and, therefore, it affects the cell coverage area by the ABS. To analyze this, the phenomenon of the interference has been described as a function of the distances between each adjacent interfering ABSs and each receiver (GS) and the PLE (path loss exponents), obtained from analyzing the data provided by the Wireless InSite ray tracing simulator. Considering the ABS positioned in the center of the interfering cells and limiting the analysis to the first tier of adjacent cells (as shown in Figure 3.11),

we have [21]:

$$SIR = \frac{S}{I} = \frac{P_{rx}}{I} = \frac{r^{-\eta}}{\sum_{i=1}^{l} d^{-\eta}} \tag{3.17}$$

where r is the distance of each receiver from its ABS, l is the number of interfering ABS, η is the PLE and d is the distance of each receiver from each interfering ABS. In this case, only six interfering ABS are assumed (*i.e.* $l = 6$) working at the same frequency on co-adjacent channels, as happens for a terrestrial scenario to compare with the existing cellular architectures. However, more than six interfering ABS can be assumed, since the base stations are moving and coverage areas eventually overlapping; moreover, the interference could be avoided using appropriate trajectories planning for the ABS.

The SINR can be calculated using [21]:

$$SINR = \frac{P_{rx}}{N + I} = \frac{SNR \cdot SIR}{SNR + SIR} \tag{3.18}$$

The considered interference scenario is shown in Fig 3.11. Here the coverage area for each ABS is clearly shown. Actually, to have interference the coverage areas should overlap but for clear understanding of the scenario, in the Figure 3.11 they have been represented as separated in order to make them clearly distinguishable.

Figure 3.12 shows the results got from the analysis of the interference phenomenon from the point of view of SINR. The attention has been put on the percentage of receivers with the SINR above the threshold at different heights , that is been set at -120 dBm for these calculations. It can be seen that the percentage of receivers with the SINR above the threshold follows a constant behavior for received power threshold kept as -120 dBm. However, it has been demonstrated that for higher thresholds, like -100 dBm and -80 dBm, the SINR tends to zero, meaning that the interference from one ABS is very high (*i.e.*

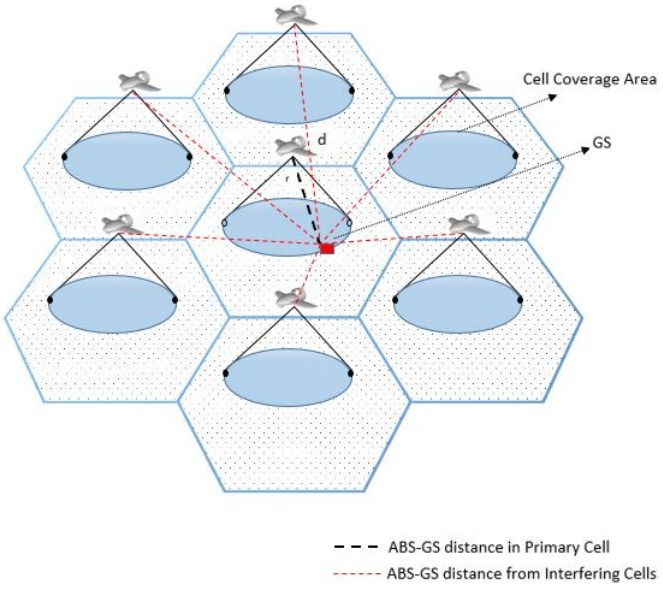

Figure 3.11: Interference scenario from interfering ABS

the received power is not enough to counteract the effect of thermal noise and interference combined so that a SINR different from zero can be obtained). For a new set of simulations with 6 interfering ABS, it has been demonstrated that the percentage decreases rapidly for a receiving threshold of -120 dBm, and still remains zero for higher thresholds. Nevertheless, since the simulations has been carried out at P_{TX}=18 dBm , it can be recognized that increasing the transmitted power is needed in order to have a better SINR for each receiver in the scenario.

3.8 Optimal Power Consumption of Aerial Base Station for Maximum Coverage

One of the most important aspect when using ABS is the amount of power they are consuming while flying. For this reason here we propose a complete power consumption analysis, taking into account both the power needed by the drone to hover P_{drone} [13], (*i.e.* the power needed for flying assuming 100%

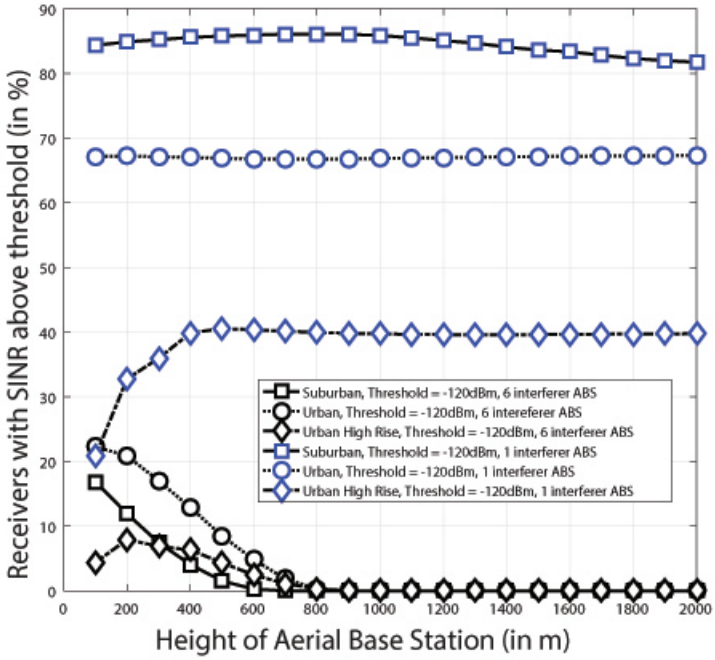

Figure 3.12: SINR analysis from an ABS at 320 m height with varying Tx power for different Rx thresholds

of efficiency) and the transmitted power P_{TX} (that is environment dependent) from the ABS to each receiver (Rx) in the environment. The expression that regulates the total power consumed $P_{consumed}$ by an ABS is:

$$P_{consumed} = P_{TX} + P_{drone} \tag{3.19}$$

$$P_{drone} = \sqrt{\frac{(2mg)^3}{16\rho A}} \tag{3.20}$$

where ρ is the density of air at sea level equal to $1.2\frac{Kg}{m^3}$), m is the mass of the drone plus payload, g is the gravitational force *i.e.* $9.8\frac{N}{Kg}$ and A is the rotor area. Hence, P_{drone} can be assumed as a constant value, since it depends only on the physical dimensions, parameters and overall weight of the drone. Therefore, the power consumed by the ABS in entirely dependent on P_{TX}, even if it has been demonstrated that the propulsion power consumption for

maintaining the UAV aloft and supporting its mobility (if necessary is usually much higher than the communication power consumption, as explained in [41].

As an example, making some assumptions it is possible to give realistic values of $P_{consumed}$ to give a better precise and detailed idea of this important aspect. For example, assuming an octocopter with a total mass (*i.e.* vehicle plus payload weight, that in our case would be the antenna weight) $m = 6Kg$ and a rotor radius $r = 0.12m$, the total area of the eight rotors will be $A = 8 \cdot (\pi r^2) = 0.362m^2$. Substituting all the values in the formula, a total power $P_{drone} \cong 27dBm$ is obtained and, consequently, assuming a transmitted power $P_{TX} = 18dBm$ for maximum coverage, a total consumed power by the drone $P_{consumed} = 45dBm$.

Chapter 4

Device-to-Device Feasibility Studies and Results

4.1 Introduction

As already said, the situation of ABS, offering connectivity to ground users in particular situations (for example earth disasters or public safety purposes) is becoming of large interest in the telecommunication field. Chapter 2 has explained how it works in details and why it is a field of big research nowadays; this type of technology offers the opportunity of discovering users that are in proximity each other's and the direct communication between them, after eNB has allowed (broadcasting SIB18 signal) them to establish a sidelink channel (SL) in between for exchanging data without routing them through the uplink and downlink channel. Moreover, three possible propagation scenarios have been proposed in Chapter 2. Here, in particular, the attention is put on the case of *partial coverage* in which many synchronization signals (*i.e.* SLSS and MIB-SL) have to be exchanged between UEs to establish a SL channel and be synchronized to get the right resources assignment, that is a high power-consumption operation from the UEs point of view; alternatively, the resources

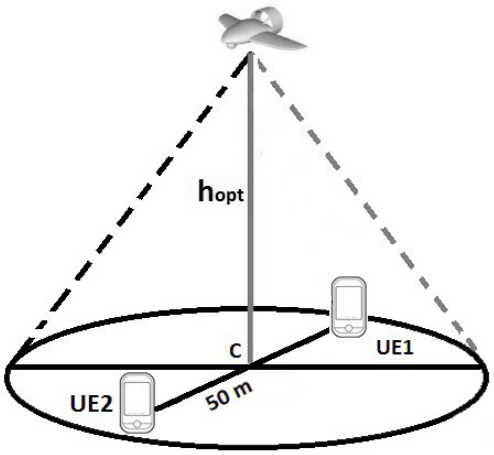

Figure 4.1: The Best Case Device-to-Device Communication

have to be preconfigured in the UEs inside the USIM, meaning that a dedicated architecture has to be used. For this reason, in this chapter, a movement of the ABS is proposed with the aim of making the UAV capable of switching from a *partial coverage* situation to a *full coverage* (*i.e.* without having the problems on the latter) is proposed.

4.2 Analysis of the Best Case D2D Communications Distance

Starting from the previous section analysis, it is possible to define the best case for a D2D communication. As the percentage of coverage radius has been calculated, it is possible to compute the measurement of the diameter D for each environment at different power level. The best case would be the one in which both the users UEs are inside the coverage area A_c. For this analysis, a transmitted power $P_{TX} = 32$ dBm is used, as commonly used in the literature for D2D communications using UAVs, see [42]. The values of the percentage of coverage area and radius for a transmitted power of 32 dBm are reported in Table 4.1.

[thr=-80 dBm]	Suburban	Urban	Urban HR
Coverage Area [%]	47 %	32 %	18 %
Radius [m]	94 m	64 m	36 m
Diameter [m]	188 m	128 m	72 m

Table 4.1: Values of coverage percentage and radius/diameter of coverage area Ac in the case of P_{TX}=32 dBm and thr=-80 dBm

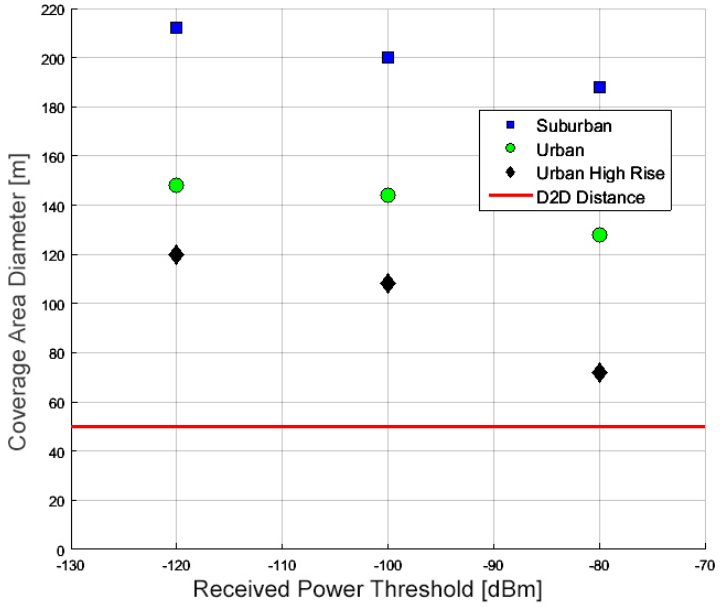

Figure 4.2: Coverage Area Diameter Values for Different Thresholds in each Environment in Best Case Situation

Starting from the diameter values, it is easy to see that they are always greater than the $d_{D2D,max} = 50m$, as explained in [35] [22], meaning that in the worst case for the distance (*i.e.* the case in which the distance between two UEs is the maximum one) it is possible to get the best D2D communication case. The best D2D cases would be all the possible combinations in which the user equipments (UEs) and the center of the Coverage Area (*i.e.* the position corresponding to the Aerial Base Station) lay on the same line; in that case, basing our analysis on the simulations results gotten, it is possible to have always a well-defined situation of *full-coverage* D2D communication.

In the other threshold cases (i.e. the cases of -120 and -100 dBm), the

[thr=-100 dBm]	Suburban	Urban	Urban HR
Coverage Area [%]	50 %	36 %	27 %
Radius [m]	100 m	72 m	54 m
Diameter [m]	200 m	144 m	108 m

Table 4.2: Values of coverage percentage and radius/diameter of coverage area Ac in the case of P_{TX}=32 dBm and thr=-100 dBm

[thr=-120 dBm]	Suburban	Urban	Urban HR
Coverage Area [%]	53 %	37 %	30 %
Radius [m]	106 m	74 m	60 m
Diameter [m]	212 m	148 m	120 m

Table 4.3: Values of coverage percentage and radius/diameter of coverage area Ac in the case of P_{TX}=32 dBm and thr=-120 dBm

behavior of the coverage percentage with respect to the transmitted power P_{TX} remains, as already said, linear but, as the power increases, the increment in the percentage of coverage area increases a few for the -100 dBm case and it remains almost constant for the -120 dBm case. Nevertheless, since the threshold is lower, the coverage percentage values for a transmitted power $P_{TX} = 32dBm$ are higher w.r.t. the -80 dBm values (as in Table 4.1). The radius and diameter values are greater in these other two cases, meaning that the best D2D communication case remains the same in which the two UEs and the ABS on the 2D plane lay on the same line. In this case they are always covered, since $d_{D2D,max} = 50m$. The value for the -120 dBm and -100 dBm are summarized in Table 4.3 and 4.2. Figure 4.2 represents the coverage area diameters w.r.t. different thresholds (-120, -100 and -80 dBm) and environment, with the aim of showing that all the values are above the D2D distance of 50 m (i.e. in all the cases the two UEs will be covered by the ABS).

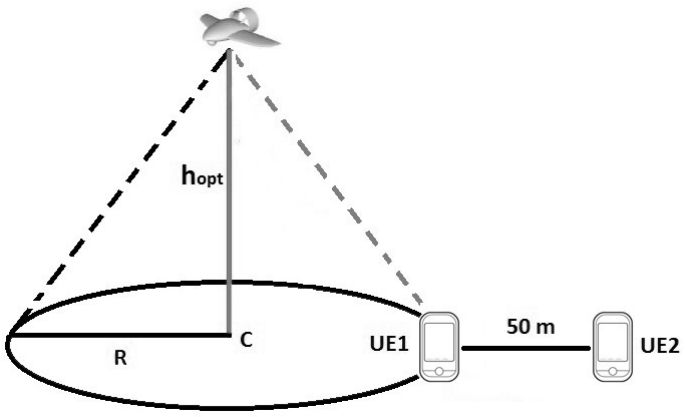

Figure 4.3: The Worst Case Device-to-Device Communication

4.3 Analysis of the Maximum Distance Covered For Different Power Levels (Worst Case)

The worst case is the one in which one user equipment is in-coverage at the border of the coverage area and the second one is out-of-coverage at a distance of 50 m. In a first analysis, it is important to understand if it is feasible to cover both the UEs, keeping the drone at the optimal height h_{opt} (since, as it has been found out, the coverage is decreasing for all the other possible values of height, as explained in 3), without moving the ABS in a different position, but simply increasing the transmitted power P_{TX}. For doing this, it is useful to start from the plot of the coverage percentage $C[\%]$ with respect to the increased transmitted power P_{TX} , available at Chapter 3. In this plot three different case of receiving thresholds are reported but the one that has more interesting conclusions is the one with receiving threshold set to -80 dBm, because it is possible to see immediately that, even if the behavior remains always linear for all the three cases, in the case of -80 dBm a rapid and monotonic increasing behavior is present, while in the case of -100 and -120 dBm the behavior is almost constant, and the percentage of coverage remains almost the same even if the transmitted power is increased till 30/32 dBm, that are commonly used

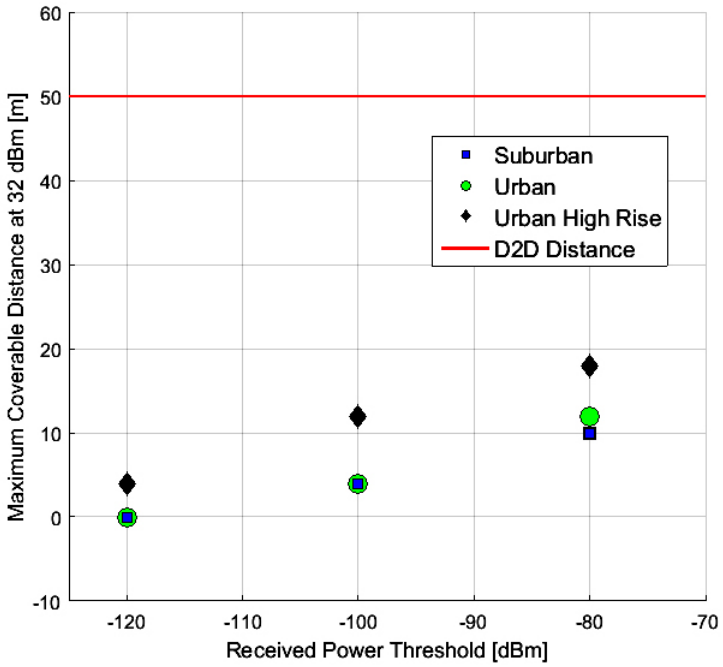

Figure 4.4: Maximum Coverable Distances for Different Environments and Thresholds increasing the Transmitted Power to 32 dBm in Worst Case Situation

and realistic values as in [42], [28].

The value of the percentage of covered area A_c, for a value of P_{TX} that goes from 18 dBm to 46 dBm, is switching from 42% to 50% in the suburban case, from 25% to 37% in the urban case and from 8% to 25% in the urban high rise. At this point, if the covered area shape is assumed to be approximated as circular (without considering any fading effect), it is possible to find the percentage of the radius of the covered area in the case of 18 dBm and 32 dBm, as the percentage of the cell radius (that was assumed to be R=200 m), getting 84, 50 and 16 meters in the case of 18 dBm and 100, 74, 50 meters in the case of 46 dBm for suburban, urban and urban high rise environment respectively. Moreover, considering the case of 18 dBm and the highest D2D-distance $d_{D2D} = 50m$ and the in-coverage UE at the border of the coverage area (*i.e.* analyzing the *worst case* where a distance of 50 m is set between the UEs) [35], it can be understood if it is possible to cover the second UE that

[thr=-80 dBm]	Suburban	Urban	Urban HR
Coverage at 18 dBm	42 %	25 %	8%
Coverage at 32 dBm	47 %	31 %	17 %
Increase in Coverage	5 %	6 %	9 %
Radius at 18 dBm	84 m	50 m	16 m
Distance to be covered	134 m	100 m	66 m
Maximum Radius Covered at 32 dBm	94 m	62 m	34 m
Is it possible to cover UEs if $P_{TX} = 32dBm$?	NO	NO	NO
Non-covered distance	40 m	38 m	32 m
$d_{D2D,max}$ coverable at 32 dBm	10 m	12 m	18 m
Movement of the ABS in meters	40 m	38 m	32 m

Table 4.4: Results on the maximum D2D-distance that can be covered by increasing the transmitted power till 32 dBm with thr=-80 dBm

is out-of-coverage simply increasing the transmitted power P_{TX} to 32 dBm (that is in principle a very high value for a aerial base station to support). By adding 50 meters to the value of radius in the case of 18 dBm, the value of distance to be covered is obtained: in this case, a value of 134, 100 and 66 meters is obtained for suburban, urban and urban high rise respectively. It is then possible to conclude that, starting from the simulation results we have, in all the cases is not possible to cover the second UE simply increasing the P_{TX}; in fact, 100 m is less than 134 m, 74 m is less than 100 m and 50 m is less than 66 m.

The same type of analysis can be done in the case of -100 or -120 dBm as threshold, but, since the increase in the percentage for covered area is very less w.r.t. the -80 dBm case (the behavior is still linear but with very low increments, especially in the case of -120 dBm as threshold), the results will be worse. The Tables 4.4, 4.5 and 4.6 summarize all the results about the worst case study that has been done for all the propagation scenarios and threshold values (*i.e.* -80, -100 and -120 dBm).

[thr=-100 dBm]	Suburban	Urban	Urban HR
Coverage at 18 dBm	48 %	34 %	21 %
Coverage at 32 dBm	50 %	36 %	27 %
Increase in Coverage	2 %	2 %	6 %
Radius at 18 dBm	96 m	68 m	42 m
Distance to be covered	146 m	118 m	92 m
Maximum Radius Covered at 32 dBm	100 m	72 m	54 m
Is it possible to cover UEs if $P_{TX} = 32dBm$?	NO	NO	NO
Non-covered distance	46 m	46 m	38 m
$d_{D2D,max}$ coverable at 32 dBm	4 m	4 m	12 m
Movement of the ABS in meters	46 m	46 m	38 m

Table 4.5: Results on the maximum D2D-distance that can be covered by increasing the transmitted power till 32 dBm with thr=-100 dBm

[thr=-120 dBm]	Suburban	Urban	Urban HR
Coverage at 18 dBm	51 %	37 %	29 %
Coverage at 32 dBm	51 %	37 %	31 %
Increase in Coverage	0 %	0 %	2 %
Radius at 18 dBm	102 m	74 m	58 m
Distance to be covered	152 m	124 m	108 m
Maximum Radius Covered at 32 dBm	102 m	74 m	62 m
Is it possible to cover UEs if $P_{TX} = 32dBm$?	NO	NO	NO
Non-covered distance	50 m	50 m	46 m
$d_{D2D,max}$ coverable at 32 dBm	0 m	0 m	4 m
Movement of the ABS in meters	50 m	50 m	46 m

Table 4.6: Results on the maximum D2D-distance that can be covered by increasing the transmitted power till 32 dBm with thr=-120 dBm

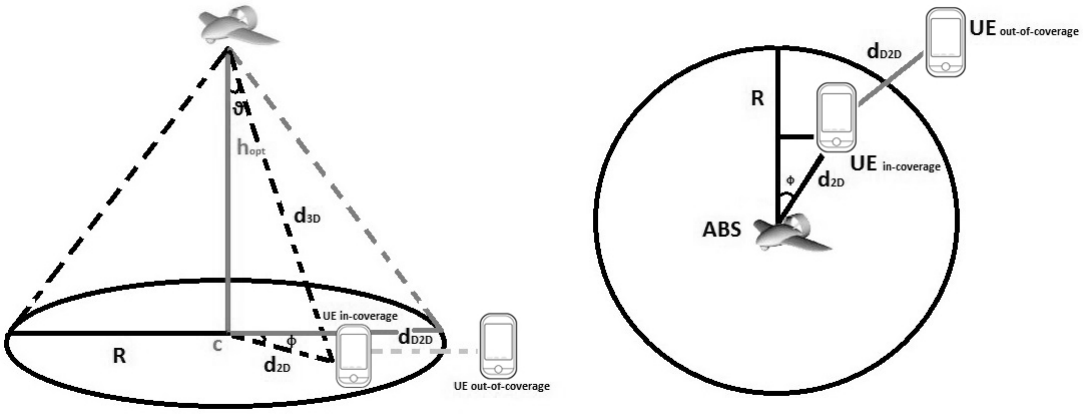

Figure 4.5: Partial Coverage situation in the case of D2D communication. 3D and 2D views.

4.4 Proposed Solution

In conventional cellular traffic using the U_u interface, the communication between eNB and UEs is achieved via UL and DL. This concept is extended in the case of D2D communications by means of the PC5 interface and the SL channel between UEs, as explained in [25]. Moreover, sender (Tx) and receiver (Rx) have to be synchronized in order to be able to correctly demodulate the transmitted data. If they are in coverage of the same ABS, there is no big problem since the receiver has just to balance the propagation delays by means of the TA (timing advance, *i.e.* the offset that the BS is assigning to each UE so that they can be synchronized when transmitting in UL). In the out-of-coverage case there is no other option apart from having preconfigured resources already inside the UEs to allow them communicating [25]. The most interesting case to analyze is the case of *partial coverage* when "the timing of both UEs are not related and the receiving UE needs additional information" [25]. As already said, in this case additional synchronization signals are needed (SLSS and MIB-SL synchronization signals) leading to less efficient operations generally. In this direction, a possible solution to this problem is proposed here to make

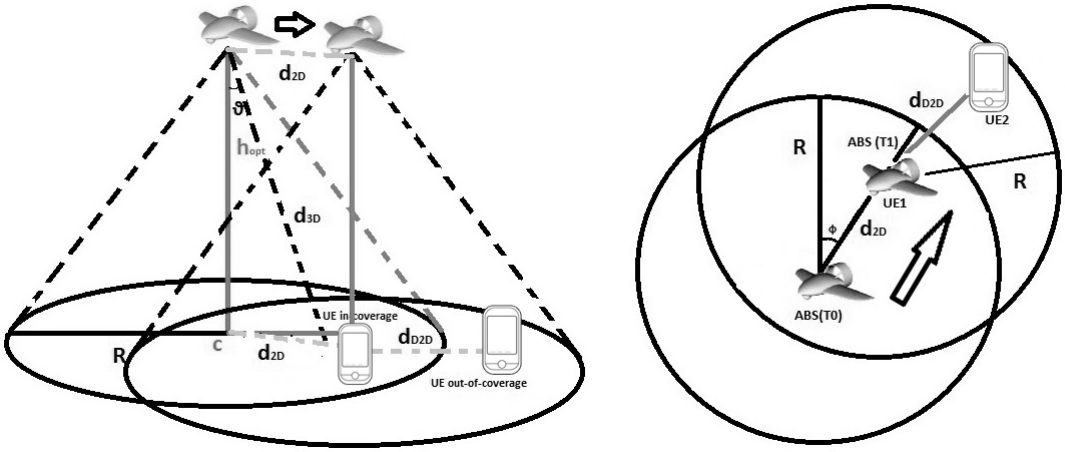

Figure 4.6: Graphical Representation of the Proposed Solution in 3D and 2D Views.

the ABS capable of switching from a situation of *partial coverage* to one of *full coverage*. The most remarkable advantages of having a full coverage situation are the following [18]:

- no additional synchronization signals (like SLSS and MIB-SL) are needed both for signaling and data exchange
- no need of having preconfigured resources inside the USIM of the UEs (*i.e.* no need of dedicated architecture services)

The basic idea of changing the position of the drone in order to switch from a partial coverage to a full coverage situation is to exploit the TA, used for compensating the propagation delay as the signal travels between the UE and eNB, ensuring that all the uplink transmissions from UEs are synchronized when received by the eNodeB (*i.e.* an UE further from the ABS will require a larger TA for compensating the larger propagation delay). Each time a UE is powered on it sends a signal to the eNB on the RACH (random access channel) for the initial access to the network when in RRC_IDLE state, for both achieving UL synchronization between the UE and the ABS and obtaining the resources for RRC Connection Request (while in the DL the synchronization

is achieved by "downlink synchronization signals" that get broadcasted to every user). After receiving RACH request, the eNB calculates the TA that is transmitted as part of the RACH response message to the user requiring the service. Moreover, it can be stated that, since the TA is somehow "a representation of the propagation time, it may be used as an approximation for TOA (time of arrival - the transmit time from UE to BS)" [34] (*i.e.* the approximated signal propagation time between the ABS and the UE), with a certain low percentage of error [19], since "each TA will correspond to a certain range of TOA values" [20] and there can be propagation phenomena bringing NLOS components and so delays in the propagation time:

$$TA \simeq TOA \tag{4.1}$$

Starting from this assumption, it is possible to define the 2D-distance d_{2D} between the UE that is in-coverage and the eNB, assuming the propagation of an E.M. signal at the speed of light c as [14]:

$$d_{2D} = TOA \cdot c \tag{4.2}$$

Moreover, if a specific estimation algorithm for the direction of arrival $DOA = (\vartheta, \varphi)$ is assumed to be available at eNB side (such as MUSIC or ESPRIT [15]) and assuming the height of the ABS as fixed at the optimal value h_{opt}, that has been found in chapter 3, the direction in which the ABS should move to switch from a partial to a full coverage situation is available. In this sense, it is possible to say that the azimuth angle φ drawn on the ground is always a constant and so the only variable in the direction of arrival (*i.e.* the direction in which the ABS has to move) is the elevation angle ϑ, that is changing point by point along the movement through the in-coverage UE position.

The solution that is proposed in this particular D2D partial coverage situation is to calculate the 2D-distance between the UE in-coverage and the center of the coverage area (where the ABS is considered to be), exploiting the TA information and the relation between the TA and the 2D-distance previously shown; then, knowing the value of the optimal height, exploiting the DOA estimation algorithm (for example using a Uniform linear array of antennas, ULA) and knowing the above mentioned 2D-distance d_{2D} (that will remain the same also on the projected circle passing through the position of the ABS), the idea is to make the ABS move of a distance value equal to d_{2D} in the direction offered by the constant azimuth angle φ. In other words, it means that it is possible to offer a full coverage D2D communication in the case of partial coverage, if the ABS is moved from the center of the coverage cell to the exact position of the in-coverage UE (at the same optimal height). It has been demonstrated that the D2D distances always stay in a specific range, as well explained in [35]and [22]:

$$5m \leq d_{D2D} \leq 50m \tag{4.3}$$

It is possible to demonstrate that almost in the 90% of the possible cases the out-of-coverage UE becomes covered by the ABS, except for the case of urban high rise environment for a threshold of -80 dBm in which the percentage of covered area is low (in fact $R_{max} = 34m < 50m$).

To demonstrate this, it is sufficient to start from percentage of coverage results with respect to the height offered in the previous section in the case of -120, -100 and -80 dBm as receiving threshold; the percentage value of cell area (of radius $R = 200mt$) and the relative percentages of radius corresponding to the the radius of the coverage area are shown in Table 4.7, 4.8 and 4.9.

So, concluding, considering the worst case of a distance of $d_{D2D} = 50m$

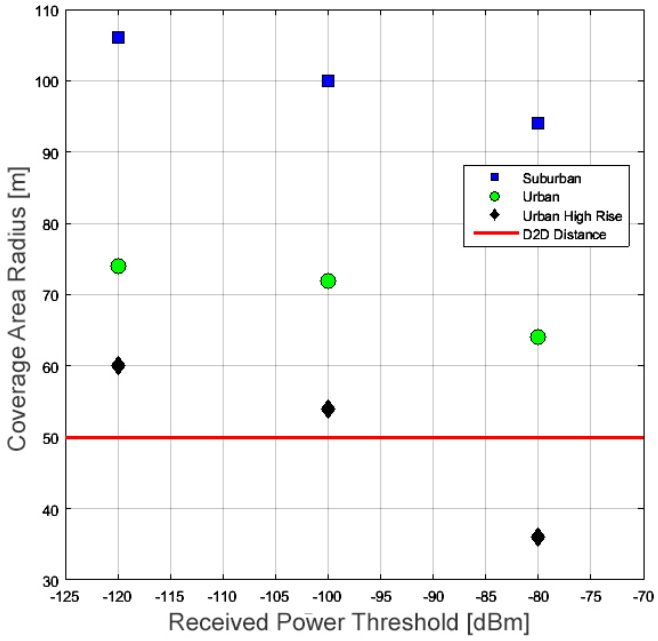

Figure 4.7: Coverage Area Radius Values for Different Thresholds in each Environment

[thr=-120 dBm]	Suburban	Urban	Urban High Rise
Coverage Area [%]	53 %	37 %	30 %
Radius of the Coverage Area	106 m	74 m	60 m

Table 4.7: Percentage value of the coverage area and relative radius values in the case of 200 m radius cell for a threshold equal to -120dBm

[thr=-100 dBm]	Suburban	Urban	Urban High Rise
Coverage Area [%]	50 %	36 %	27 %
Radius of the Coverage Area	100 m	72 m	54 m

Table 4.8: Percentage value of the coverage area and relative radius values in the case of 200 m radius cell for a threshold equal to -100 dBm

[thr=-80 dBm]	Suburban	Urban	Urban High Rise
Coverage Area [%]	47 %	32 %	18 %
Radius of the Coverage Area	94 m	64 m	36 m

Table 4.9: Percentage value of the coverage area and relative radius values in the case of 200 m radius cell for a threshold equal to -80 dBm

between the two D2D UEs, if the ABS takes the same position of the in-coverage-UE, this position turns out to be the new center C of the coverage area A_c, that is not changing in absolute value since the value of the height is the same. Finally, since the value of the radius in different environments is always greater than 50 m except for one case, basing the analysis on our calculation and simulations results, it is possible to say that in the 90% of the cases the second UE will be covered by the ABS (just one case over nine will have a maximum $d_{D2D,max} = 34m$), switching the partial-coverage case to a full-coverage, with all the advantages of the case (see Figures 4.5 and 4.6 for better understanding).

4.5 Final Considerations

It has been demonstrated that, in case of a *drone-assisted D2D communication*, an optimal and worst case can be identified. The first case is represented by two UEs that are 50 m distant (*i.e.* the maximum D2D distance) and lay on the same line passing through the center of the coverage area A_c. It is shown that in all the different scenarios and threshold levels the diameter is always greater than 50 m. The second one, instead, is the case in which again a distance equal to 50 m is again present between two UEs but one of them is under the coverage of the ABS (the in-coverage UE) at the border of the coverage area and the second one (the out-of-coverage UE) is not. In this case, instead, results show that even increasing the transmitted power P_{TX} from 18 to 32 dBm is not enough to cover the out-of-coverage UE and in that case it is necessary to move the ABS in a different position. The last part of the analysis is dealing with an ABS movement proposal to switch from a partial-coverage situation to a full-coverage, in which there is no need of synchronization signals between UEs and no need of having preconfigured resources in the USIM of

the UEs. In this direction, a new solution is proposed: the idea is that of using and exploiting the TA as a possible approximation of the TOA to calculate the d_{2D} and then to use a $DOA = (\vartheta, \varphi)$ estimation algorithm so that the drone knows in which direction to move and the value of the distance to be traveled. It is shown that in the 90% of the cases this solution is working and the situations of partial-coverage turn out to be transformed into a full-coverage situation. Finally, it is important to underline the fact that the results can present a small percentage of error, even if it has been demonstrated that all the simulations results of the software Wireless Insite well approximate the reality, as explained in [27].

Conclusions

It is possible to state that the topic regarding base stations (BS) mounted on UAVs (such as drones or small airplanes) is becoming a field of big interest in the telecommunications area. Many companies like Nokia [7], Qualcomm [8], Ericsson, China Mobile [3] and Huawei [5] are investing a lot in this field. In the past literature few papers are available on this topic, such as [31], [38]. Nevertheless, these papers are touching similar topics even if the actual approach they are using is simply analytical. In this direction, this thesis brings novelty, since all the analysis have been done starting from a well cited ray tracing simulator. The first part of the work is centered on the coverage, capacity and interference analysis of an aerial base station (ABS). Using a CAD software three different propagation scenarios have been created (suburban, urban, urban high rise) following the ITU-R specifications. Then simulations in three different environments have been performed at different height from 100 m to 2000 m with a value of the transmitted power $P_{TX} = 18dBm$. Then, the coverage analyses using a receiving threshold equal to -120 dB have been performed for all the scenarios, calculating the integral over the cell area of the product of the distance between each user equipment (UE) and the aerial base station (ABS) by the probability for each UE of receiving a power greater or equal to the threshold; a common range of the optimal height has been found between 300 m and 400 m. Moreover, the relation between an increment in the transmitted power and the effect on the coverage for different environment

and receiving thresholds has been given. The next proposed results refer to the capacity analysis that have been computed using the Shannon formula involving the SNR and the bandwidth of the signals. Next step of the work has been to analyze the case in which the first tier of six interfering ABSs is considered (assuming that they are working at the same frequency and on co-channels) considering the air-to-ground channel model in the case of different propagation environments as a function of distance and path-loss exponents; the results have been expressed in terms of SNR and SINR. Last but not least, a complete power consumption analysis including both the power needed to the drone to fly and the transmitted power of the ABS is done.

The second part of the thesis focuses on the possibility of using ABS for a drone-assisted D2D communications between ground users. Starting from the percentage coverage results w.r.t. the transmitted power level available at Chapter 3, some feasibility studies have been done, considering a realistic value of transmitted power equal to 32 dBm. First, an optimal and worst case is individualized, considering the maximum possible value for the D2D-distance between the users equal to 50 m. The optimal case turns out to be the one in which both the users equipment and the ABS lay on the same line passing through the center of the coverage area. It has been demonstrated that, with the obtained simulation results, the UEs are always in-coverage of the ABS. The worst case is, instead, the one in which one UE is in-coverage at the border of the coverage area and the second one is out-of-coverage at a distance of 50 m. It has been demostrated that, even incrementing the transmitted power level to 32 dBm, it is not possible to switch from a partial to a full-coverage situation in all the environments. The attention is finally put to the case of *partial-coverage* in which many synchronization signals (*i.e.* SLSS and MIB-SL) have to be exchanged between UEs to establish a sidelink channel and be synchronized to get the right resources assignment that is an high power-consumption operation

for the UEs; alternatively, the resources have to be preconfigured in the UEs inside the USIM, meaning that a dedicated architecture has to be used. For this reason, a movement of the ABS is proposed in this thesis, to switch from a partial to a full-coverage situation like no one has proposed before (in fact, some optimization problems are available, like [24] but only from a statistical or analytical analysis). The idea is to exploit the timing advance information available to the eNB and considering it as a possible approximation of the TOA to get the value of the 2D-distance d_{2D} between the position of the ABS and the in-coverage UE, considering the propagation of an E.M. field at the speed of light. Assuming then a DOA estimation algorithm available at eNB side, it is demonstrated that in the 90% of the cases it is possible to switch from a partial to a full-coverage situation moving the ABS in the exact position of the in-coverage UE at distance d_{2D} previously calculated in the direction offered by the DOA.

Regarding the possible future work, the possibility of including the movement of the UAV and the UEs in the simulations could give a more detailed analysis of the work, allowing to understand if the results are reflecting the reality or not. Moreover, a detailed analysis of the consequences and effects of the doppler effects due to the movements of both the UEs and the UAV could be a great improvement for the work.

Bibliography

[1] "LTE sidelink resource pools and PSCCH period", available at https://it.mathworks.com/help/lte/examples/lte-sidelink-resource-pools-and-pscch-period.html, accessed May 2017.

[2] www.autodesk.it/products/3ds-max/overview.

[3] www.ericsson.com/en/news/2016/8/ericsson-and-china-mobile-conduct-worlds-first-5g-drone-prototype-field-trial-.

[4] www.g-uav.com/en/index.html.

[5] www.huawei.com/en-nz/events/mwc/2017/all-cloud-network/5g/lets-get-5g-up-and-running.

[6] "www.lteinwireless.blogspot.it/2011/06/all-about-sibs-in-lte.html".

[7] www.networks.nokia.com/products/connecteduavs.

[8] www.qualcomm.com/invention/technologies/lte/advanced-pro/cellular-drone-communication.

[9] www.remcom.com/wireless-insite-em-propagation-software.

[10] "Propagation data and prediction methods required for the design of terrestrial broadband millimetric radio access systems operating in a frequency range of about 20-50 ghz". *Rec. ITU-R P.1410-2*, 2001.

[11] "Aerial Base Stations with opportunistic links for unexpected and temporary events". *Next Generation Public Safety Systems*, 2015.

[12] S. Lardner A. Al-Hourani, S. Kandeepan. "Optimal LAP altitude for maximum coverage". *IEEE Wireless Communications Letters*, 2014.

[13] Rhett Allain. "Physics of the Amazon Octocopter drone", available at https://www.wired.com/2013/12/physics-of-the-amazon-prime-air-drone/, accessed November 2016.

[14] Kaveh Pahlavan Bardia Alavi. "Modeling of the TOA-based distance measurement error using UWB indoor radio measurements". *IEEE Communications Letters*, 2006.

[15] Kung Yao Chiao En Chen, Flavio Lorenzelli. "Stochastic maximum-likelihood DOA estimation in the presence of unknokn nonuniform noise". *IEEE Transaction On Signal Processing*, Jul 2008.

[16] Pramod Viswanath David Tse. *"Fundamentals of Wireless Communication"*. Cambridge University Press, 2004.

[17] Gerhard P. Fettweis Fred Richter, Albrecht J. Fehske. "Energy efficiency aspects of base station deployment strategies for cellular networks". *Vehicular Technology Conference Fall*, 2009.

[18] S.Sorrentino P.Wallentin Q. Lu N. Brahnmi G. Fodor, S. Parkvall. "Device-to-Device communications for national security and public safety". *IEEE Access*, 2014.

[19] Shankari Panchapakesan George P. Yost. "Errors in Auomatic Location Identification using Timing Advance". *VTC IEEE*, pages 1955–1958, 1998.

[20] Shankari Panchapakesan George P. Yost. "Improvement in estimation of time of arrival (TOA) from Timing Advance (TA)". *IEEE*, pages 1367–1372, 1998.

[21] Andrea Goldsmith. *"Wireless Communications"*. Cambridge University Press, 2005.

[22] Chengwen Xing Haichuan Ding, Shaodan Ma. "Feasible D2D communication distance in D2D-enabled cellular networks". *IEEE ICCS*, 2014.

[23] National Telecommunication Information, editor. *"Telecommunications: Glossary of Telecommunications Terms"*. National Telecommunication Information.

[24] Rui Zhang Teng Joon Lim Jiangbin Lyu, Yong Zeng. "Placement optimization of UAV-mounted mobile Base Stations". *IEEE Communications Letters*, 21(3), Mar 2017.

[25] A.Roessler J.Schlienz. "Device to Device communication in LTE". *White paper*.

[26] Durgaprasav Palepu Latha P V. "Device to Device communication in LTE". *Sasken*, Jun 2016.

[27] Blagojevic Zeljko Mededovic Petar, Veletic Mladen. "Wireless Insite software verification via analysis and comparison of simulation and measurement results". *Proceedings of the 35th International Convention MIPRO*, 2012.

[28] Faraj Lagum Halim Yanikomeroglu Mohamed Alzenad, Amr El-Keyi. "3D placement of an Unmanned Aerial Vehicle Base Station (UAV-BS) for energy-efficient maximal coverage". *IEEE Wireless Communications Letters*, May 2017.

[29] Mehdi Bennis Mohammad Mozaffari, Walid Saad. "Efficient deployment of multiple Unmanned Aerial Vehicles for optimal wireless coverage". *IEEE Communications Letters*, 20, Aug 2016.

[30] Mehdi Bennis Merouane Debbah Mohammad Mozaffari, Walid Saad. "Unmanned aerial vehicle with underlaid device-to-device communications: Performance and tradeoffs". *IEEE Transactions on Wireless Communications*, 2015.

[31] Mehdi Bennis MÃšrouane Debbah Mohammad Mozaffari, Walid Saad. "Unmanned aerial vehicle with underlaid device-to-device communications: Performance and tradeoffs". *IEEE Transactions on Wireless Communications*, Feb 2016.

[32] Ian Poole. "D2D communication for high data rate local direct communications using LTE devices", available at www.radio-electronics.com/info/cellulartelecomms/lte-long-term-evolution/4g-lte-advanced-d2d-device-to-device.php, accessed May 2017.

[33] S. Rangan T.A. Thomas A. Ghosh I.Z. Kovacs I. Rodriguez O. Koymen A. Partyka J. Jarvelainen S. Sun, T. S. Rappaport. "Propagation path loss models for 5G urban micro- and macro-cellular scenarios". *VTC Spring*, pages 1–6, 2016.

[34] Khalid G. Samarah. "Localization of mobile stations from one base station in GSM systems". *International Review on Computers and Software*, May 2016.

[35] Janne Lehtom Timo Koskela Sami Hakola, Tao Chen. "Device-to-Device (D2D) communication in cellular network - Performance analysis of optimum and practical communication mode selection". *IEEE WCNC*, 2010.

[36] Jonathan Rodriguez Shahid Mumtaz. *"Smart Device to Smart Device Communication"*. Springer, 2014.

[37] Satoshi Nagata Qun Zhao Shinpei Yasukawa, Hiroki Harada. "D2D communications in LTE-Advanced Release 12". *NTT Docomo Technical Journal*, 2015.

[38] Falko Kuester Tom Wypych, Radley Angelo. "AirGSM: An Unmanned, flying GSM cellular Base Station for flexible field communications". *IEEE Aerospace Conference*, 2012.

[39] Sathya Narayana Venkatasubramanian. "Propagation channel model between unmanned aerial vehicles for emergency communications". Master's thesis, Aalto University, 2013.

[40] Amitabha Ghosh Rapeepat Ratasuk Xingqin Lin, Jeffrey Andrews. "An overview of 3GPP Device-to-Device proximity services". *IEEE Communications Magazine*, 2014.

[41] Rui Zhang Yong Zeng. "energy-efficient uav communication with trajectory optimization". *IEEE Transactions on Wireless Communications*, 2017.

[42] Pavel Mach Jan Plachy David Gesbert Zdenek Becvar, Michal Vondra. "Performance of mobile networks with UAVs can flying Base Stations substitute ultra-dense small cells?". *23rd European Wireless (EW)*, May 2017.